PROGRESS REPORT

BASIC FAILURE MECHANISMS IN ADVANCED COMPOSITES

prepared for

NATIONAL AERONAUTICS AND SPACE ADMINISTRATION

by

J. V. Mullin, V. F. Mazzio and R. L. Mehan

October 1971

CONTRACT NASw-2093

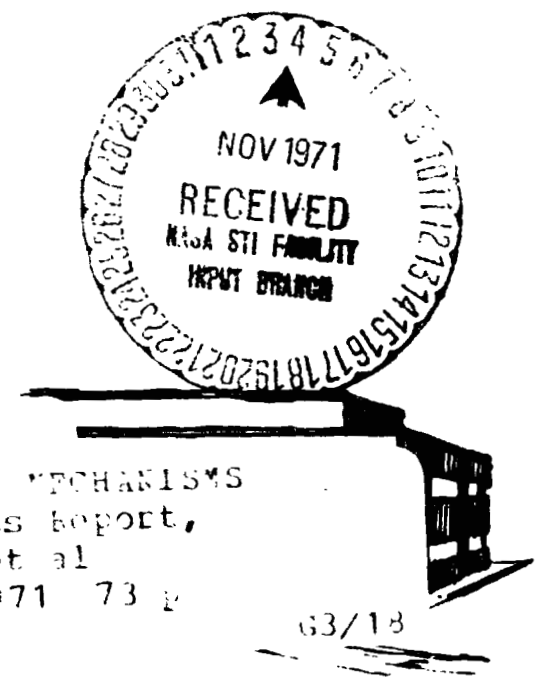

Space Sciences Laboratory
Space Division
GENERAL ELECTRIC COMPANY
Philadelphia, Pa.

2420-N03 (PROGRESS REPORT)

PROGRESS REPORT

MAY THROUGH OCTOBER 1971

BASIC FAILURE MECHANISMS IN ADVANCED COMPOSITES

BY

J.V. MULLIN, V.F. MAZZIO AND R.L. MEHAN

PREPARED FOR

NATIONAL AERONAUTICS AND SPACE ADMINISTRATION

OCTOBER 1971

CONTRACT NASw-2093

SPACE SCIENCES LABORATORY
GENERAL ELECTRIC COMPANY
SPACE DIVISION

TABLE OF CONTENTS

LIST OF ILLUSTRATIONS

LIST OF ILLUSTRATIONS (CONT'D)

LIST OF TABLES

SUMMARY

This progress report covers the period from 25 April 1971 to 25 October 1971; the work is being performed under Contract NASw-2093 with Mr. Bernard G. Achhammer as Program Monitor.

The purpose of the program is to identify fundamental failure mechanisms in carbon-epoxy composites as a basis for more reliable prediction of the performance of these materials. Following the approach established under a previous contract (NASw-1543) and building on the progress made last year, single and multiple fiber specimens were tested under tensile loads and the sequence of failure events was observed. Parameters such as resin crack sensitivity, fiber surface treatment and variations in fibers from batch to batch are being evaluated. This year's effort also includes the analysis of bulk composite fracture processes using acoustic emission techniques in an attempt to correlate microscopic observations with bulk composite behavior.

Other aspects of the program include attempts to control the fracture process through matrix and interface modification and the study of failure processes in composite/metal specimens. Although most of the effort described here involved DEN 438 epoxy novolac as the matrix, some experiments are now underway using the higher temperature resin ERLA 4617.

By carefully examining fiber/matrix interactions during the failure process we hope to gain the insight necessary to reconstruct the entire failure process in bulk composites, thus improving over ability to design more efficiently with these materials.

SECTION 1

INTRODUCTION

The research described herein is an outgrowth of efforts initiated under NASw-1543 where failure mechanisms in boron/epoxy were investigated. In the first year of the current efforts emphasis was shifted to carbon fibers with the major focus on matrix and interface response to fiber fracture. Comparisons were made between different fibers, various fiber surface treatments and different degrees of matrix crack sensitivity. In each case the approach was to first identify basic fracture mechanisms in single and multiple fiber specimens and then to explore means for controlling the failure process to prevent sudden catastrophic failure. The validity of such an approach depends on how translatable are the observations to the case of a heavily reinforced composite. Therefore bulk composite specimens have been fabricated and tested to evaluate the more significant differences in behavior observed in the microscopic studies. Unfortunately, there are few characterization techniques which allow the systematic and detailed monitoring of the basic elements in the failure process in such specimens. This need has led to the monitoring and analysis of acoustic emissions from the bulk composites during the entire load history. Although the use of acoustic emission equipment to monitor structural behavior under load is well known, the use of the technique in this study is more fundamental to understanding material performance. Specific failure mechanisms and sequences of events in the failure process which can be controlled and identified acoustically are of primary concern.

A part of the current effort will also be applied to the study of failure mechanisms in composite/metal specimens because of their increased use. Both flat sandwich specimens and tubes of carbon/epoxy bonded to aluminum alloy are now being fabricated for this phase of the program. Preliminary efforts and specimen descriptions will be included in this report.

The research described here is fundamental in nature but essential to the accurate prediction of composite material performance. Only through an understanding of the failure process can we hope to design reliably with fiber-reinforced composites. Further, this understanding will contribute to improved inspectability through a knowledge of the sequence of events which presage final failure of a composite part.

SECTION 2

MATERIALS CONSIDERATIONS

2.1 FUNDAMENTAL FAILURE MECHANISMS

In the past, two modes of local failure have been observed in the fracture surfaces of composites: fiber fracture and fiber pullout. The first mode is essentially fiber limited while the second suggests that insufficient bonding was available to fracture the fiber. Unfortunately, in a densely packed composite the degree to which the two modes are discernible depends on how tortuous the failure process is and the nature of the fibers themselves.

This points up the desirability of observing the local failure process in very simple specimens. Since carbon fibers are used in tow form, the interaction between individual filaments within the tow and the overall response of the tow are both of major concern in establishing basic failure mechanisms. We are concerned here with the first evidence of failure in the fibers and the role which the matrix plays in propagation of these initiated cracks.

First experiments [1] were performed on boron/epoxy specimens and three distinct failure sources were observed to occur in the matrix at the fiber fracture site. These are illustrated in Figure 1 and can be summarized as follows:

1. In the upper picture the filament has remained strongly bonded to the matrix on either side of the break. This results in the disk-shaped crack normal to the fiber which grows suddenly; its size is determined by the magnitude of the strain energy released when the fiber fails.

2. When the filament is not so strongly bonded to the matrix, the high shear stress concentrations at the interface adjacent to the fiber break can cause unbonding to occur. This is illustrated in the center photo of Figure 1 where the boron filaments had been coated to obtain such behavior.

3. If the bond strength is sufficient but the matrix is weak in tension, a tensile crack may propagate in the high shear transfer region beginning at the interface and growing at about 45^{o} to the fiber axis at its source as shown in the lower photo of Figure 1. Note that this crack becomes nearly normal to the fiber axis as it propagates. This is consistent with the nature of the tensile stress field around the fiber break as determined photoelastically by several earlier studies (2, 3).

Analysis of such failure mechanisms can help to discern whether a particular fiber/matrix combination is fiber, matrix or interface limited. However, because only isolated fibers are being observed, we have, at best, only an indication of the elements which contribute to the failure of bulk composites. Therefore the approach is to examine both single and multiple fiber interactions in simple specimens and then to correlate these data with the fracture process in heavily reinforced specimens. In this way the effects of matrix modification, fiber surface treatment, and the like on composite performance can be more readily understood.

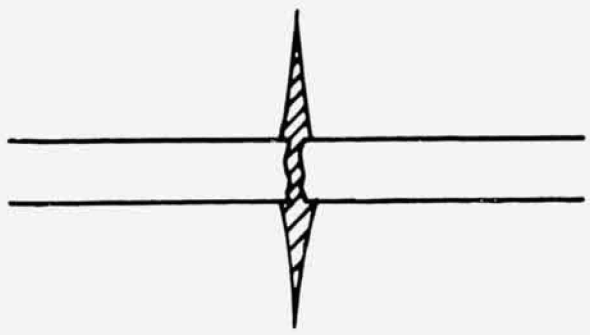

HIGH ENERGY RADIAL
CRACK NORMAL TO FIBER

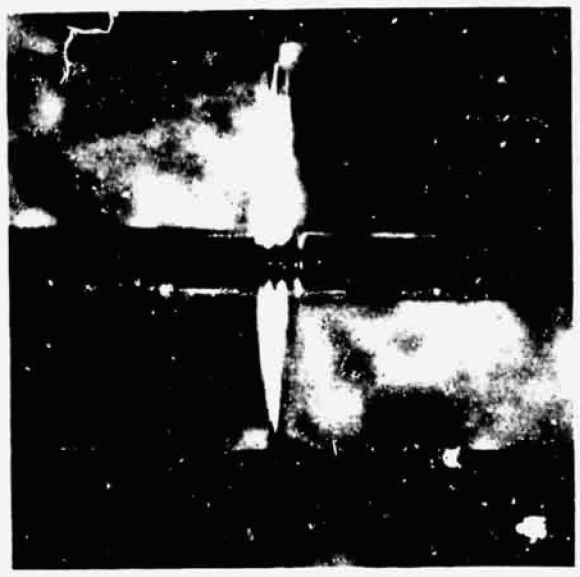

INTERFACE UNBONDING DUE TO HIGH
SHEAR STRESS AT NEWLY FORMED
ENDS

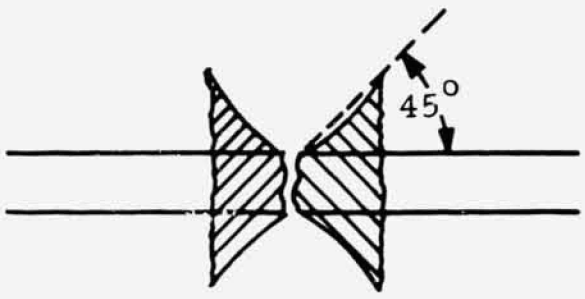

LOW ENERGY RESOLVED SHEAR
STRESS INDUCED TENSILE
CRACKS IN THE MATRIX

Figure 1. Diagrams and Photographs of Failure Mechanisms in Boron-Epoxy

2.2 NATURE OF THE FIBERS

2.2.1 MECHANICAL PROPERTIES

Of the various commercially available high-strength, high-modulus carbon fibers, treated and untreated Type A and HT fibers were selected for study in this phase of the program. Type HM fibers - treated and untreated - are on hand for future work. It was felt that these three carbon fibers are most commonly used and cover a range of strength and stiffness characteristics. Besides the fundamental properties of the fibers, there are the additional considerations of surface chemistry and morphology which can affect the wetting and bonding characteristics and, therefore, the bond strength. In every instance experiments were undertaken on a comparative basis in an attempt to isolate the effects of a single variable.

During the past year major emphasis was focused on evaluating untreated fibers because it was planned to modify the interfacial bond strength in order to control the fracture process. The untreated fibers provide an excellent reference base for this purpose. Even though interlaminar shear strength values have been improved by oxidative surface treatments, the effects on other properties are still not completely understood. Composites made with treated fibers have shown some strength deterioration after a period of time and this problem is of major concern. Therefore, a comparison of the mechanical response of treated and untreated fibers represented a significant part of the work reported here as did fiber variation from one batch to another.

Advanced fibers come in multi-fiber tow form ranging from 48 inches to 3,000 feet long without splices. Tows contain approximately 10,000 individual fibers which average about 8 microns in diameter. The number of fibers, varying lengths and their extremely small diameter present some handling difficulty as far as fiber spacing and orientation are concerned. Tows of Type A and HT fibers used during the course of this work were reduced to small numbers in simple specimens. In this instance, fiber handling and specimen preparation was made more difficult because the fibers, being extremely lightweight, have a tendency to move about freely when placed in a heated resin matrix during processing. This fiber movement sometimes results in specimens ranging from a loose distribution of fibers to a compacted bundle with some fiber crossover.

The properties of the Type A and HT fibers used in this work, along with those to be used later in the program, are shown in Table 1.

2.2.2 SURFACE CHARACTERISTICS

Since the time of their discovery, the structure of high-strength carbon fibers has received much attention. Some of the areas studied by others were surface morphology, porosity, and wetting characteristics. The physical structure of carbon fiber surfaces is of considerable importance in determining the interfacial area available for bonding between fiber and matrix in a composite. Estimates of pore size and shape in carbon fibers can be obtained from x-ray scattering data (4, 5) and electron microscopy (4). The technique used in the present program is electron microscopy. The surfaces and structures of PAN-based and α-cellulose-based fibers, covering a wide range of moduli and strength, were examined. The series of figures following is presented to show a comparison between two lots of untreated HT fibers; designated original and new, and untreated versus treated HT and Type A fibers.

Table 1. Manufacturer's Fiber Test Data

Fiber Type & Batch No.	Date Rec'd	Ten. Str., x 10^3 psi	Ten. Mod., x 10^6 psi	Filament Dia.
Original HT	7-69	387	37.1	7.4*
HT-U (New) (PPH 42/124)	7-71	379	39.1	8.1*
HT-S (New) (PT117/201Z)	9-71	364	36.0	8.3*
Type A (Original) (PPC53/733)	1-71	346	29.5	8.1*
Type A (New) (PA1/19)	7-71	315	28.5	8.4**
Type A-S (New)	7-71	326	28.9	8.6*
HM (Original) Courtauld's Type B	None	375	55	8.2*
HM-S (New) (QM123/306W)	9-71	296	62.5	7.4**

*Used to date
**To be used later in the program

The original untreated HT fiber surface is shown in Figure 2a at 30,000x. At this magnification the surface appears only slightly rough with occasional pit marks and irregular edges. By comparison the new untreated HT fiber surface shown in Figure 2b at 30,000x appears to be somewhat smoother, with no marks but some irregularity along the fine edges. In general, however, there is no significant difference in surface characteristics.

The treated HT fiber surface, on the other hand, shown in Figure 3 at 30,000x appears to have many more surface irregularities and imperfections along the fiber surface than the untreated fibers.

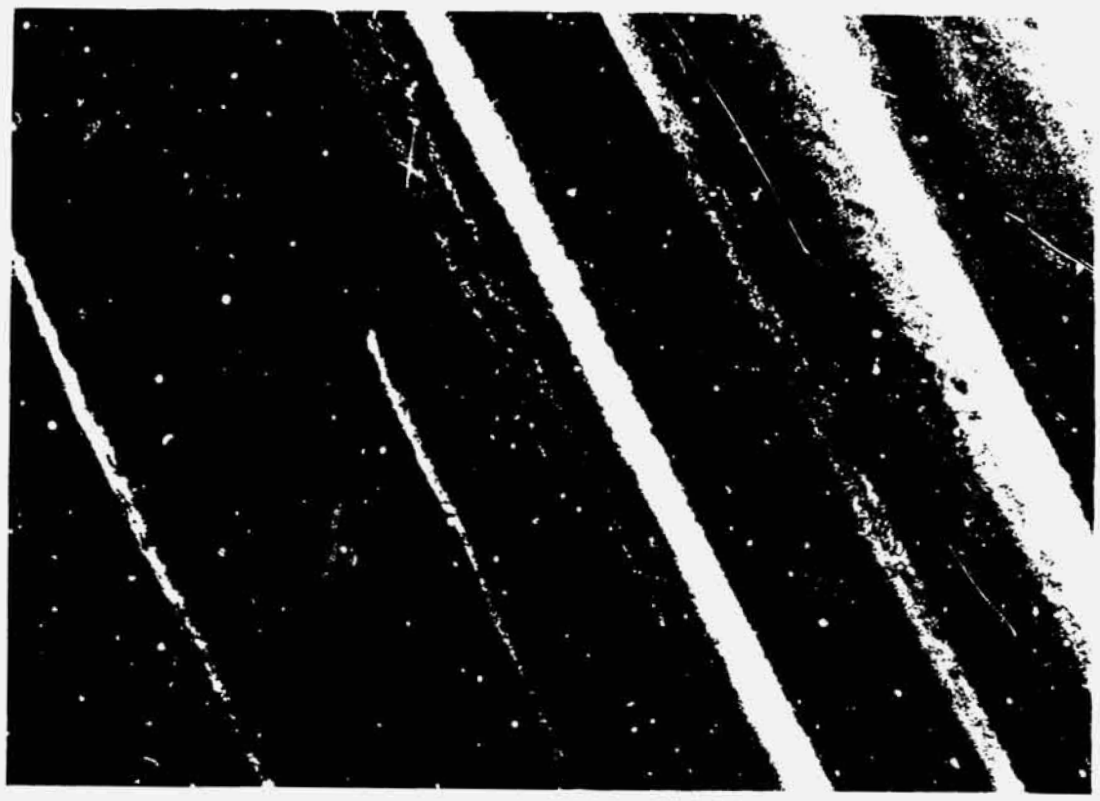

a) Original Untreated HT Carbon Fiber Surface - 30,000 X Mag.

b) New Untreated HT Carbon Fiber Surface - 30,000 X Mag.

Figure 2. Comparison of Surface Characteristics of Two Batches of Untreated Carbon Fibers

Figure 3. Photomicrograph of Surface Treated HT-S Fibers (30,000 X)

A third comparison is made between Type A untreated and treated fibers. It can be observed in Figure 4a that the surface appears smooth and possesses a well-oriented graphitized structure with the main fiber axis. The treated Type A fiber surface shown in Figure 4b at 30,000x is rough and pitted along the edges of the fibrils.

In summary, electron micrographs of the fiber surfaces indicate a smoother surface on the untreated fibers (both HT and Type A) compared to the treated fibers. Comparing HT fibers from two separate batches (original and new) we see no appreciable difference. It appears then that besides any chemical changes that might occur as a result of surface treating the fibers, there are some physical changes which might enhance bonding. However, these changes are not extreme.

2.3 MATRIX CHARACTERISTICS

The principal functions of the matrix in any composite system is to transfer stress to the fibers and isolate fiber fractures. When the matrix is capable of being modified without degrading its load transfer function, one can develop the toughness and flexibility to prevent rapid and catastrophic crack propagation.

2.3.1 MECHANICAL PROPERTIES

Considering toughness and flexibility to be important control parameters, two epoxy systems were selected for study. The first is DEN-438, an epoxy-novolac resin produced by Dow Chemical Company. It is one of the first and widely used epoxy-type resins having good strength and modulus, and it can be easily modified to provide improved toughness and elongation. The second is a cycloaliphatic epoxy resin designated ERL4617, which has 20% higher strength and 100% higher modulus than most other epoxies.

The DEN-438 system is cured with NMA (Nadic Methylanhydride) and BDMA (Benzyl Dimethylamine) is used as the accelerator. PPG-425 (Polypropylene Glycol) is used as the flexibilizer to impart additional toughness and elongation. Shortcomings of the flexibility are that the Anhydride curing agent and PPG flexibilizer significantly reduce the elevated temperature mechanical properties, and the PPG, although a Co-reactant, is hygroscopic causing reduced strength under high humidity conditions. However, for structural applications at ambient temperatures, the system is excellent. The properties of the epoxy-novolac formulations - unmodified and modified - are shown in Table 2. Note that the toughness of the modified resin is higher by a factor of three, while elongation is greater by an order of magnitude. Tensile strength and modulus suffer greatly from modification, and this can be expected to have a more significant effect on transverse properties.

The unmodified DEN 438 matrix system, being an inherently brittle system, can be extremely crack sensitive in uniaxial tension in single and multi-filament composites depending on the fiber strength, bond strength and load rate. In some cases incremental uniaxial tensile loading shows no cracking or debonding until the ultimate load is reached. At this point a single crack may appear, and will often cause catastrophic failure. On the other hand, the modified formulation allows small cracks to accumulate at lower load levels. The ductility of the resin in the modified sense is therefore beneficial to absorbing energy released when each

a) Untreated Type "A" Carbon Fiber Surface - 30,000 x Mag.

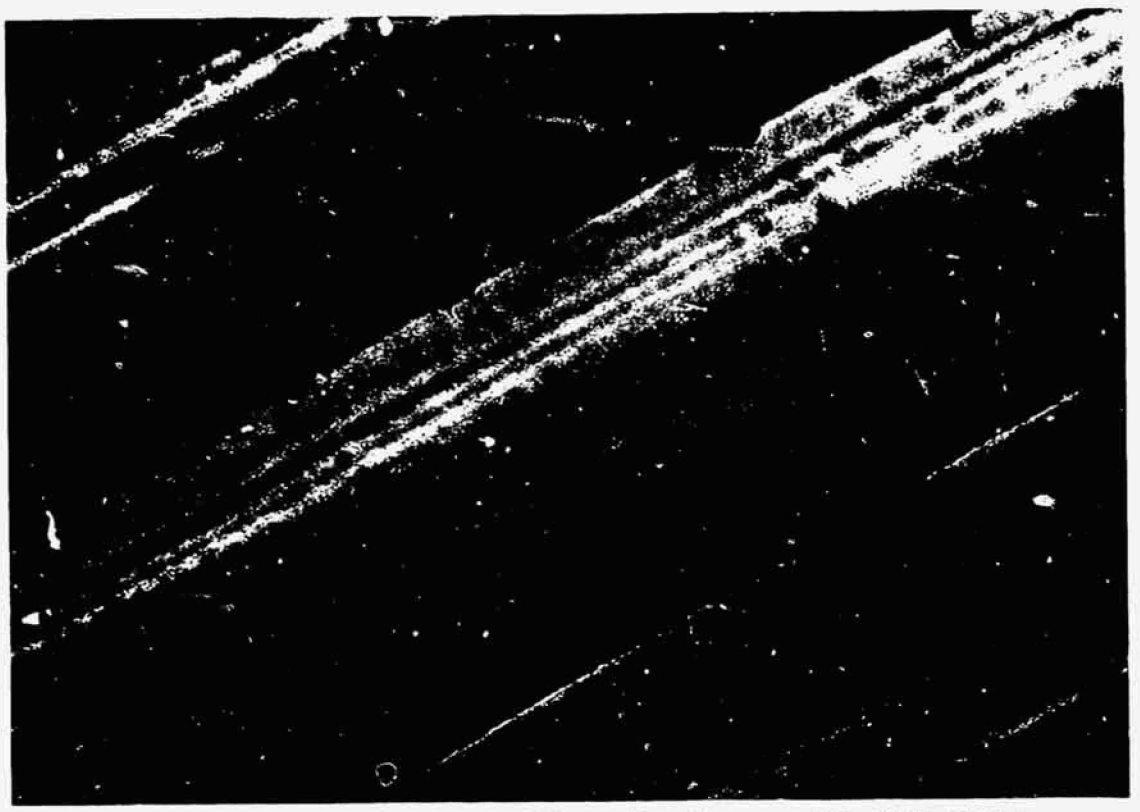

b) Treated Type "A" Carbon Fiber Surface - 30,000 X Mag.

Figure 4. Comparison of Surface Characteristics of Untreated and Treated Type "A" Fibers

fiber breaks, and containing the crack with each occurrence until gross damage occurs. Arridge (6) has shown that toughness is an important parameter in fiber reinforced composites but suggests that in a real composite the flexible or toughened matrix acts like a rigid system because of fiber constraint.

Table 2. Properties of Epoxy-Novolac Formulation

	Unmodified	Modified
FORMULATION:	DEN 438 - 100 PBW MNA - 72 PBW BDMA - 2 PBW	DEN 438 - 100 PBW MNA - 72 PBW PPG 425 - 60 PBW BDMA - 2 PBW
PROPERTY:		
Ultimate Tensile Strength, x 10^3 psi	- 6.5 - 10	- 3.7 - 4.5
Modulus of Elasticity, x 10^6 psi	- 0.40 - 0.45	- 0.20 - 0.25
Elongation, %	- 2.5	- 15 - 25
Toughness, in. lb/$in.^3$	- 150 - 250	- 650 - 700
Specific Gravity	- 1.22	- 1.21

Another consideration is the difference in modulus between the matrix system and fibers. The ratio of fiber modulus to that of the matrix is so great (100:1) that modulus is not an important matrix parameter in uniaxial tension compared to toughness and total elongation. In transverse tension the situation is not the same however. Under this load condition high matrix strength and modulus are often required. The problem of mechanical compatibility is immediately evident under different loading conditions, and suggests that a great deal still has to be done to optimize a combination of matrix properties in order to achieve greater composite performance.

Properties of the ERL 4617 system are shown in Table 3. Here the difference in properties relate to the different curing agents used with each formulation. ERLA/m-PDA and ERLB, MDA have quite different toughness and elongation properties but only slight difference in modulus. This system is more opaque than the epoxy novolac system but with careful control of lighting clear pictures of the local fracture patterns can be obtained.

2.3.2 SHRINKAGE CHARACTERISTICS

All resins systems, regardless of chemical structure or molecular configuration, shrink during the cure and post-cure cycle as well as upon cooling to room temperature. Post-cure shrinkage is caused by molecules rearranging into a compact structure or in the particular case of condensation resins, by the evolution of lower molecular components during cure. Cool-down shrinkage is simply due to the effects of temperature on atom spacing. Our

concern is in the former case in working with epoxies during the preparation of single and multiple fiber specimens. Non-uniform shrinkage places single strands and individual fibers in a stressed condition which can result in fiber crimping and/or debonding. There is greater chance of shrinkage in the flexibilized system and, therefore, different curing techniques have to be used to minimize this condition. A modification of the mold setup was made in order to reduce shrinkage and fiber crimping. This is outlined in the next section.

Table 3. Properties of Cycloaliphatic Epoxy Formulations

FORMULATION:	ERLA 4617-114.0 PBW M-PDA-Curing Agent 27.0 (PBW)	ERLB 4617-114.0 PBW MDA Curing Agent 43.0 (PBW)
PROPERTY:		
Ultimate Tensile Strength x 10^3 psi	20	16-20
Modulus of Elasticity x 10^6 psi	0.815	0.78
Elongation, %	2.8	6-7
Toughness, in. lb/in.^{3}	320	832
Specific Gravity, gms/cc	1.27	1.26

2.4 SPECIMEN PREPARATION AND TESTING

2.4.1 SINGLE AND MULTIPLE SPECIMENS

In the case of the epoxy-novolac resin the cure cycle and mold configuration were the main parameters to consider for achieving uniform matrix properties and good fiber orientation from specimen to specimen. The single and multiple fiber composite specimens were prepared according to the following procedure.

1. A shallow 4 inch square mold assembly with 1 inch square brass rods, spaced 1/4 inch apart, was coated with a thin film of RAM 225 mold release agent. The solvent was evaporated out of the RAM at room temperature. The film was then baked onto the mold for one hour at 250°F to provide a stable film which will not diffuse into the matrix during cure.

2. A thin layer (1/16 inch) of epoxy resin was poured into the mold and partially cured (effectively "B" staged) as follows:

   1 hour at 180°F for the unmodified system; 2 hours at 180°F for the modified system.

   This rendered the resin sufficiently tacky to prevent fiber movement during final cure.

3. After the first cure, the filaments were laid down parallel with one another, at the desired spacing. Additional epoxy (1/16 inch) was poured over the filaments.

4. The composite, regardless of matrix state, was then cured for 2 hours at 180°F followed with a stepwise increase in temperature to 350°F at which point post-cure was carried out for 2 hours.

5. The specimens were removed from the mold, sanded to desired thickness and polished.

Some work was started during this reporting period with the ERLA 4617 cycloaliphatic epoxy resin system cured with MDA (methylenedianiline). Gelatin time ("B" staging) for the first 1/16 inch layer was carried out for 4 hours at 200°F. The resin was fairly well gelled, but it was noted that shrinkage began to occur as soon as the resin began to cool. Fibers were placed on this layer immediately, and another 1/16 inch layer of resin was applied over the fibers. The assembly was then placed in the oven again for final cure for 4 hours at 250°F plus 16 hours at 325°F.

The Cycloaliphatic system is more reactive than the epoxy-novolac resin making the working time shorter and less reproducible from batch to batch. Newer techniques are being explored for handling this system in simple low fiber volume specimens.

All simple specimen tests were conducted at the same strain rate (0.02 in./in./min). To obtain a complete picture of the fracture events to ultimate failure it was necessary to interrupt the test at regular intervals for thorough microscopic examination. This introduces some complications since the interruption of the failure process may in itself introduce extraneous effects which would not occur under continuous loading. However, the lack of sufficient magnification and scanning control on a machine mounted microscope dictated this approach. All tests were carried out on an Instron testing machine with complete recording of load and deformation.

Microscopic examination was carried out on a Bausch and Lomb microscope for the most part with magnifications between 20 and 300x. The details of the failure process for various test parameters are presented in Section 3.

2.4.2 HIGH VOLUME FRACTION SPECIMENS

Additional high fiber volume tensile specimens were prepared and tested, containing a new batch of untreated HT carbon fibers to obtain more information for the unmodified and modified epoxy-novolac systems. This was done because fundamental differences were observed in behavior from the original fibers in single and multiple fiber tests. Since unmodified and modified resin was used and the quantity involved was small, wet prepregging and curing was done by hand in place of using commercially available prepreg materials. Some specimens were prepared from the original batch of HT fibers to obtain higher volume fraction data since the original bulk composite data had resulted in relatively low fiber volume fractions and the effect of this difference was a major parameter to be evaluated.

Briefly, the process used for preparing all high volume fraction specimens with both resin systems was to immerse a preweighed amount of fibers in the matrix and place the bundle in a 9 inch long x 0.5 inch wide mold, then pre-staging in a circulating air oven for a prescribed time (45 minutes at 180°F for the modified system and 20 minutes at 180°F for the unmodified system). This was followed by placing the male section of the mold on the prepreg, placing the assembly in a press and curing for 2 hours at 180°F, followed by a stepwise increase in temperature to 350°F and held for 2 hours.

The specimens were removed from the mold, cleaned of mold flash, tabbed on the ends with 1 1/2 inch x 0.5 inch Scotchply 1002 tabs and tested in an Instron testing machine at a strain rate 0.02 in./in./min. The results of these tests are discussed in Section 3.1.2.

SECTION 3

EXPERIMENTAL PROCEDURES AND OBSERVATIONS

3.1 UNTREATED FIBER FAILURE MECHANISMS

Because the interfacial bond strength is a critical factor in the reinforcing process all previous experiments were performed on untreated fibers. This provided a useful basis for comparison with subsequent interface control studies. Except for comparisons between different types of fibers, primary emphasis was placed on the high performance HT fibers obtained from Courtaulds in 1969 and these have the designation "original" in the following discussion. In July of 1971 a new batch of untreated HT fibers was obtained from Hercules Inc. having the designation "new" with properties essentially the same as discussed previously. Since the failure mechanisms for these two batches of the same kind of fiber show discernible differences in single and multiple fiber failure mechanisms, this section will be devoted to a comparison of both the microscopic observations and bulk composite properties for the two batches of fibers.

3.1.1 SINGLE AND MULTIPLE FIBER BEHAVIOR

Following the procedures established in earlier experiments, tensile specimens were prepared with a small number of carbon fibers encapsulated in both modified (15 to 25 percent strain to failure), and unmodified resin (2.5 percent strain to failure). The fracture mechanisms observed in the unmodified resin are shown in Figure 5. The upper photo shows typical behavior of the original batch of fibers where no accumulation of fiber fractures was evident and the first fiber fracture resulted in failure of the specimen. There was no evidence of fiber pullout or debonding which indicates that the bond was strong.

The lower photo in Figure 5 shows the typical behavior of the new batch of untreated HT fibers in the unmodified resin system. Although the failure was essentially the same with only one matrix crack, there was evidence of fiber pullout near the fracture. This is evident in the lower photo of Figure 5 and suggests some difference in the interfacial bond strength between the two batches of fibers when tested in the same resin system. A comparison of the two batches of untreated HT fibers in the modified resin system shows even more dramatic differences in the fracture modes. The upper photos in Figure 6 shows how the original batch of fibers initiated disk-shaped cracks normal to the fibers as they failed in tension. By contrast, the lower photo shows no such cracks even when clear separation of fibers indicates that fracture has occurred. Since the resin tends to rebound after loading and close these separations, it is difficult to photograph these fiber fractures which don't crack the matrix. Their presence is substantiated by the large debonded areas observed along the length of the fibers and the fracture strain of the specimen which greatly exceeded that of the fibers.

This difference in interfacial behavior between two batches of the same fiber cannot be attributed to surface morphology since microscopic examination at 30,000 X shows no visible difference in surface characteristics as shown in Figure 2. To determine whether

(a) Original Untreated HT Fibers in Unmodified Resin-60 X

(b) New Untreated HT Fibers in Unmodified Resin - 60 X

Figure 5. Comparison of Two Batches of Untreated HT Fibers in Unmodified Resin

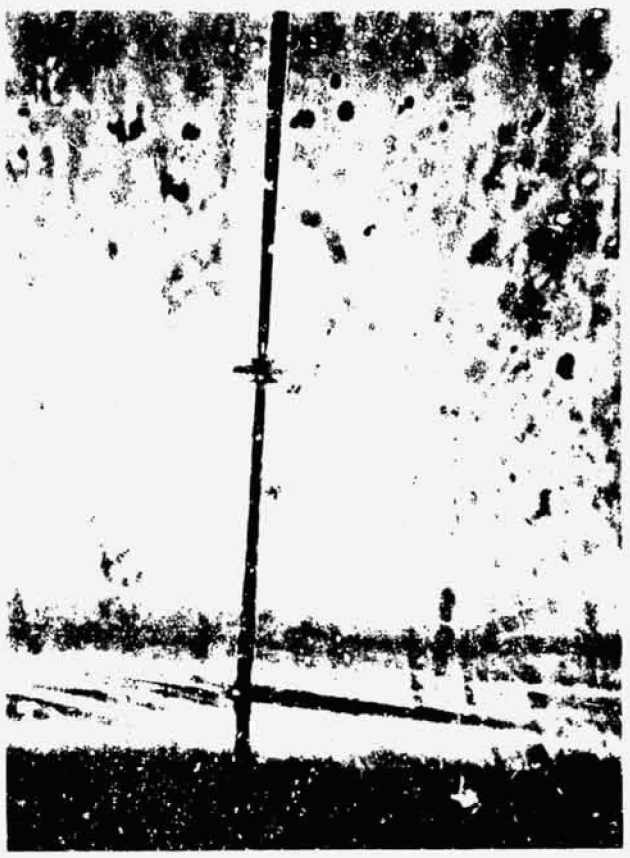

150 X

28 X

Original HT Fibers in Modified Resin

300 X

28 X

New HT Fibers in Modified Resin

Figure 6. Comparison of Two Batches of Untreated HT Fibers in Modified Resin (Arrows Indicate Fiber Fractures and Matrix Cracks)

this difference in microscopic behavior would affect bulk composite properties a series of tensile specimens were prepared and tested for comparison with the bulk data obtained earlier with the original batch of fibers. The results of these tests are discussed in the following section.

3.1.2 BULK COMPOSITE PROPERTIES

Tensile specimens of the new batch of untreated HT fibers were prepared and tested using the same procedures and specimen geometry as had been used with the original HT fibers. Table 4 shows the data obtained for each batch of fibers in both modified and unmodified resin. Figure 7 is a plot of tensile strength versus volume fraction for all data obtained on untreated HT fibers. The data from specimens containing the fibers from the original batch are shown as triangles with open triangles representing modified resin and solid triangles representing unmodified resin. Note that there was considerable variation in the fiber volume fraction of specimens made from the original batch with values ranging from 0.20 to 0.55. No obvious effect of matrix modification is evident in the data and the lower line represents a reasonable fit. Some of the scatter in these data is due to improvements in the specimen preparation technique with the very low volume fraction specimens having been prepared earlier. It should be noted here that because untreated fibers were being studied, specimens were prepared by impregnating individual tows and hot pressing after hand lay-up in a matched metal dye mold. This procedure generally gives less uniformity than the use of prepreg tape where fiber orientation and resin content are much more critically controlled.

The circles in Figure 7 represent the tensile strength data for the new batch of fibers in both the unmodified and modified epoxy resin. Even though the strength data reported by the manufacturer is very nearly the same for each batch, the composite strength with the newer fibers is noticeably higher than that of the original batch for equal volume fractions of fibers. The scatter in the test data for the new batch of fibers is also less than that obtained for the specimens made with the original batch. One might expect to obtain greater scatter at lower volume frctions but even if we ignore the data below a 0.40 fiber volume fraction, the difference in scatter is obvious and cannot be attributed solely to improved processing of specimens. In an attempt to gain further insight into the reasons for this difference in mechanical behavior, gross fracture modes were studied for all the tensile specimens.

First we will compare the fracture modes as a function of volume fraction in the unmodified resin system. In Figure 8 the upper photo shows typical fracture modes obtained with the original fibers in first specimens prepared during last year's research efforts. During the first month of this year's effort more specimens were prepared and tested using the same fibers but with higher volume fraction of fibers. These are shown in the lower photo of Figure 8. Note that the fracture mode at the lower volume fraction (upper photo) is still cleavage but now it occurs on several planes which are linked at final failure by fracture planes parallel to the load axis (along the specimens). This latter observation cannot be attributed to a change in interfacial behavior since the same batch of fibers and resin formulation were used in the two sets of specimens. This point is further reinforced by by the fact that no fiber pullout was observed and this is consistent with previous results

Table 4. Comparison of Tensile Strength Data for Two Batches of Untreated HT Carbon Fibers in Both Unmodified and Modified Epoxy-Novolac Resin

Unmodified Resin (Original Fibers)				Modified Resin (Original Fibers)			
Spec. No.	Tensile Strength, psi	Tensile Mod; x 10^6 psi	V_f	Spec. No.	Tensile Strength, psi	Tensile Mod; x 10^6 psi	V_f
HTR-1	41,400	8.23	0.21	HTF-1	138,000	21.6	0.56
HTR-2	32,000	10.0	0.26	HTF-2	55,100	19.6	0.51
HTR-3	36,200	9.85	0.25	HTF-3	56,500	12.1	0.31
HTR-5	55,000	13.0	0.33	HTF-5	60,000	12.0	0.31
HTR-6	74,000	11.9	0.31	HTF-6	90,000	12.7	0.33
HTR-7	93,500	15.0	0.39	HTF-7	99,000	18.9	0.49
HTR-8	111,000	16.2	0.42	HTF-8	114,000	18.0	0.47
HTR-9	88,700	13.0	0.33	HTF-9	58,500	13.5	0.35
HTR-10	68,500	14.2	0.37	HTF-10	61,600	13.6	0.35
HTR-11	95,000	19.5	0.50	HTF-11	108,000	15.5	0.40
HTR-12	130,000	19.5	0.50	HTF-12	87,200	14.5	0.37
Avg.	75,030			Avg.	84,355		
	Unmodified Resin (New Fibers)				Modified Resin (New Fibers)		
HTUR-1	171,000	21.9	0.55	HTUF-1	149,000	18.5	0.47
HTUR-2	162,000	19.8	0.50	HTUF-2	120,000	17.5	0.44
HTUR-3	157,000	22.0	0.56	HTUF-3	130,000	25.0	0.63
HTUR-4	139,000	19.6	0.50	HTUF-4	139,000	20.0	0.51
HTUR-5	148,000	19.1	0.48	HTUF-5	143,000	17.8	0.45
HTUR-6	134,000	18.9	0.42	HTUF-6	140,000	18.4	0.47
				HTUF-7	159,000	22.0	0.56
				HTUF-8	131,000	17.3	0.44
Avg.	151,830			Avg.	138,875		

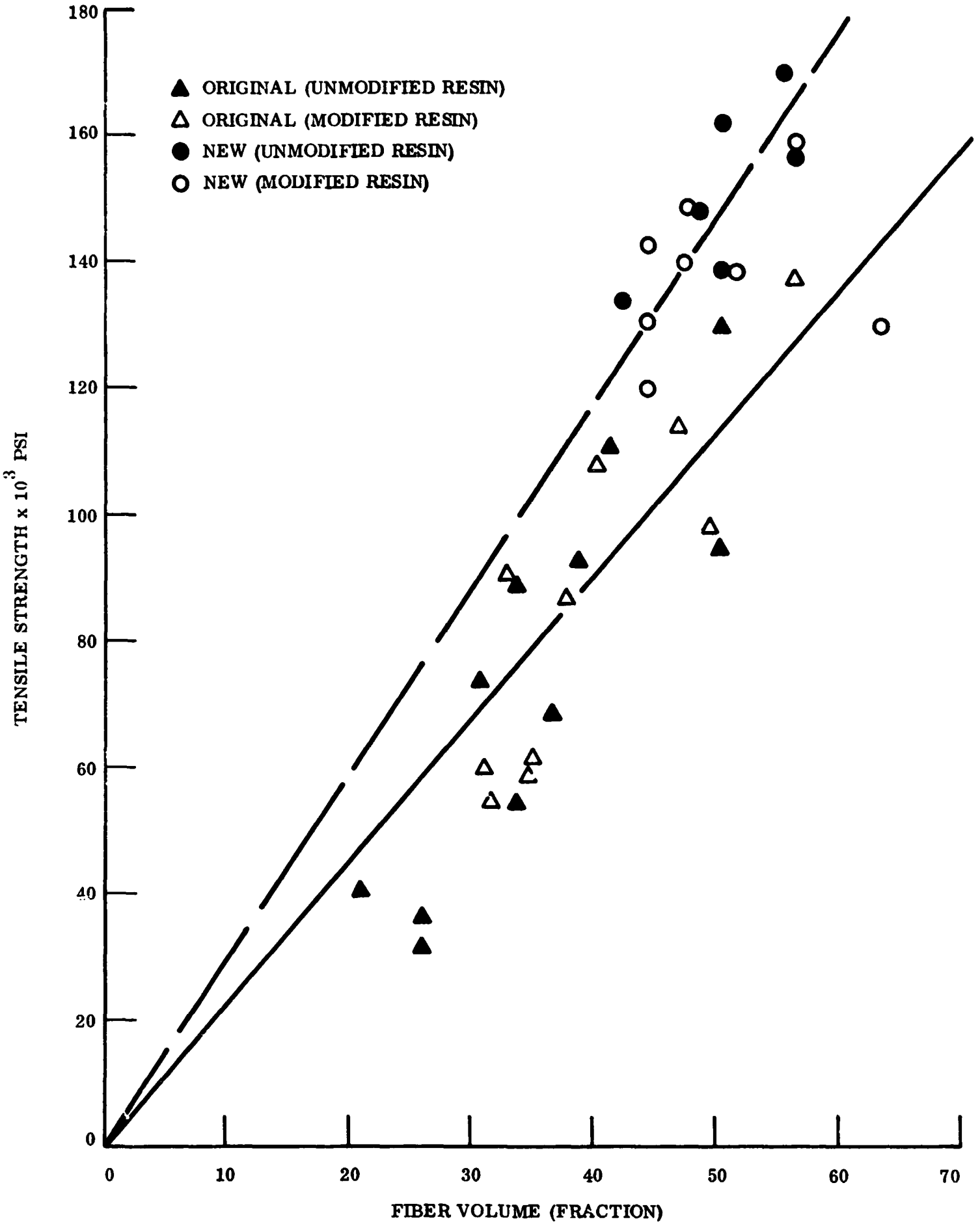

Figure 7. Tensile Strength Data Comparison for Two Batches of HT Carbon Fibers in Both Modified & Unmodified Epoxy Resin

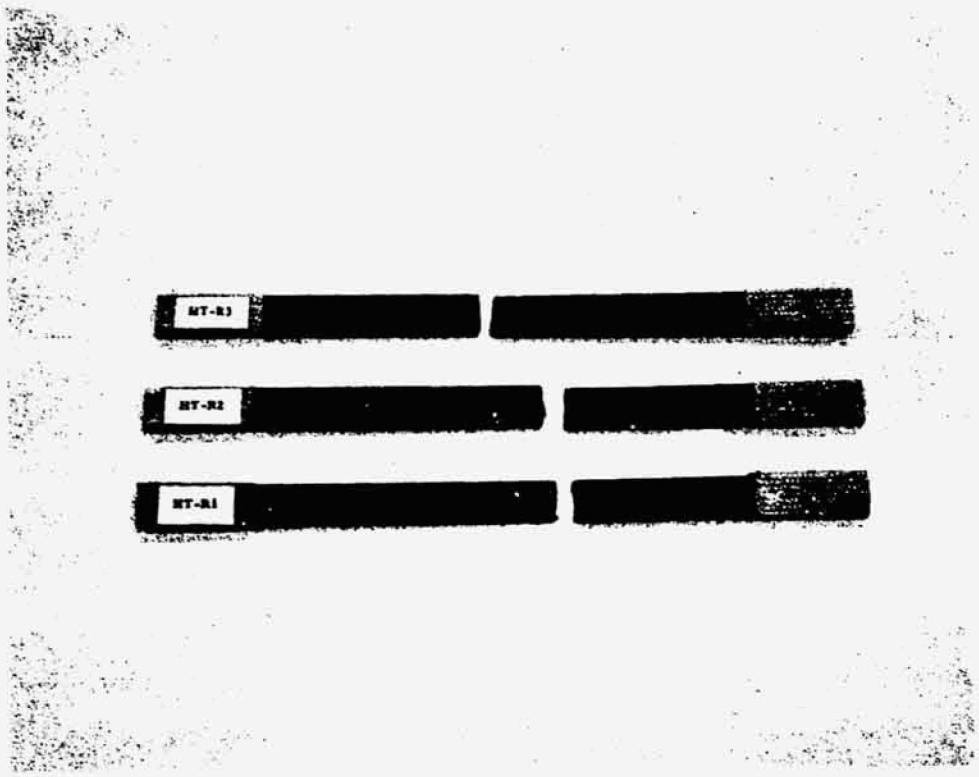

V_f	σ_c x 10^3 psi	E x 10^6 psi
.25	36.2	9.9
.26	32.0	10.0
.21	41.4	8.3

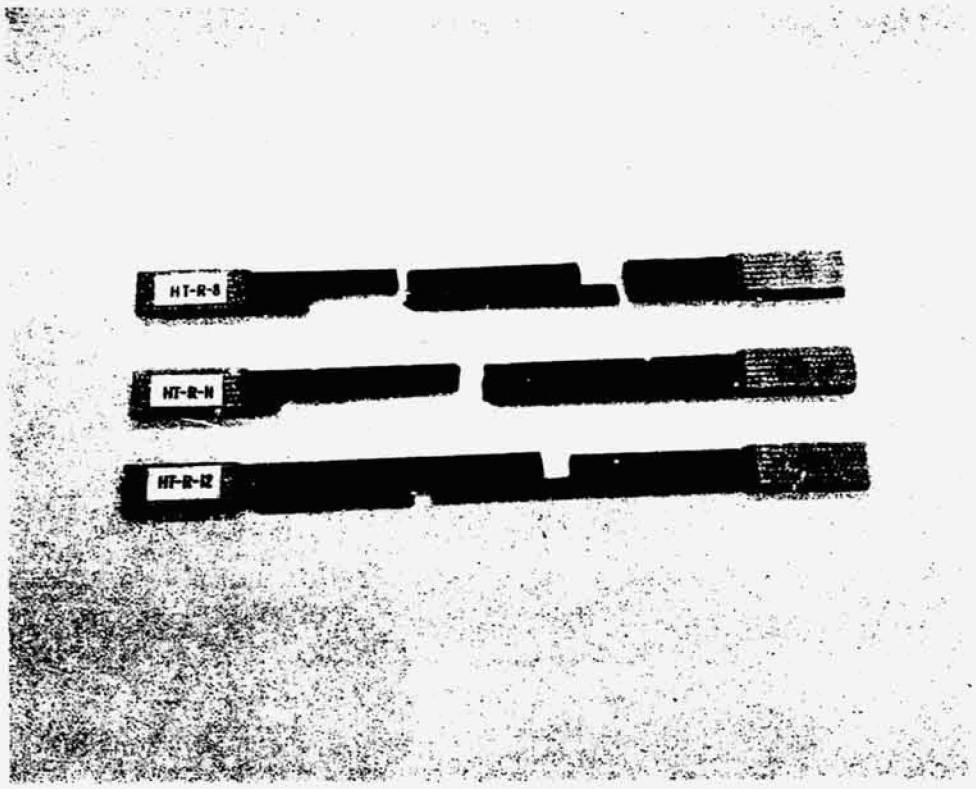

V_f	σ_c x 10^3 psi	E x 10^6 psi
.42	111.0	16.2
.50	95.0	19.5
.50	130.0	19.5

Figure 8. Comparison of Gross Failure Modes as a Function of Fiber Volume Fraction for Original Fibers in Unmodified Resin

in single fiber specimens. It appears that the more closely packed the fibers, the less the matrix crack sensitivity of the unmodified resin influences the initiation and growth of a single critical crack. This would seem to agree with the model proposed by Hedgepeth [7] in which the matrix is assumed to be capable only of carrying shear to adjacent fibers.

Figure 9 shows a comparison of two different batches of fibers in the same unmodified resin system with the upper photo typical of fracture modes with the original batch of fibers. Care was taken to compare similar volume fractions and this is the same photo discussed previously in Figure 8. The lower photo shows the specimens fabricated from the new batch of fibers and considerably less cleavage with a good deal of transverse separation of fibers and fiber pullout. This again is consistent with the observations discussed previously in single fiber and tow specimens. Note that damage extends over a large portion of the specimen in most cases. The average strength of the newer batch specimens was 30 to 50 percent higher than those fabricated from the old batch. This resulted in much more energy released at final failure and, therefore, we must be careful not to confuse post-test damage due to stress waves with the basic fracture patterns.

Figure 10 shows a similar comparison in the modified epoxy resin formulation with the gross fracture modes quite similar to those shown previously for the unmodified resin. Although the cleavage with the original batch of fibers (upper photo) is not as distinct as it was in the unmodified resin, this is still the dominant mode of failure. The new batch of fibers on the other hand, behave quite differently with very little cleavage and a good deal of fiber pullout and transverse splitting. The most notable difference here is the greater scatter which occurs with the original fiber specimens (where cleavage is significant) compared to t hat of the newer fiber specimens (where cleavage is not widespread). Since this scatter is evident even between specimens having nearly the same volume fraction of fibers, it appears that the cleavage failure mode in either modified or unmodified resin is a very random failure process. The more tortuous behavior of the specimens made from the newer batch of fibers showed less scatter, higher strength and, therefore, more predictable behavior.

3.2 TREATED FIBER FAILURE MECHANISMS

All previous discussion has centered on untreated fibers because they provided a convenient reference point for further study of interface behavior. The greater volume of fibers used in prepreg systems for structural applications have surface treatment and therefore a series of experiments has been undertaken to evaluate the influence of surface treatment on failure mechanisms. The following sections will describe microscopic failure mechanisms for HT and Type A treated fibers inepoxy novolac and some preliminary data in the ERLA 4617 resin system. Properties for each resin system have been presented earlier in Section II.

3.2.1 SURFACE TREATED HT FIBER BEHAVIOR

The use of a surface treatment is intended to enhance the bond strength between the carbon fiber and the matrix. Since the bond strength with untreated fibers was already sufficient to break the fibers in tension, one might expect that only subtle differences in failure

Original Fiber 1st Batch

V_f	σ_c x 10^3 psi	E x 10^6 psi
.42	111	16.2
.50	95	19.5
.50	130	19.5

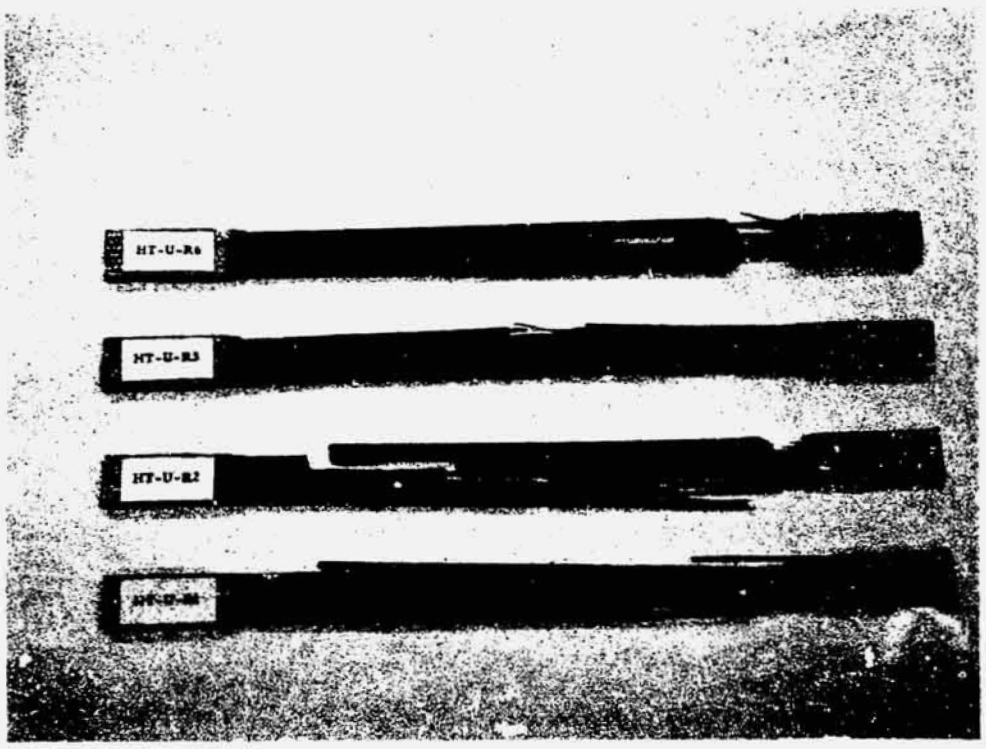

New Fiber Batch

V_f	σ_c x10^3 psi	E x10^6 psi
.42	134	18.9
.56	157	22.0
.50	162	19.8
.55	171	21.9

Figure 9. Comparison of Gross Failure Modes for two Batches of HT Fibers in Unmodified Resin

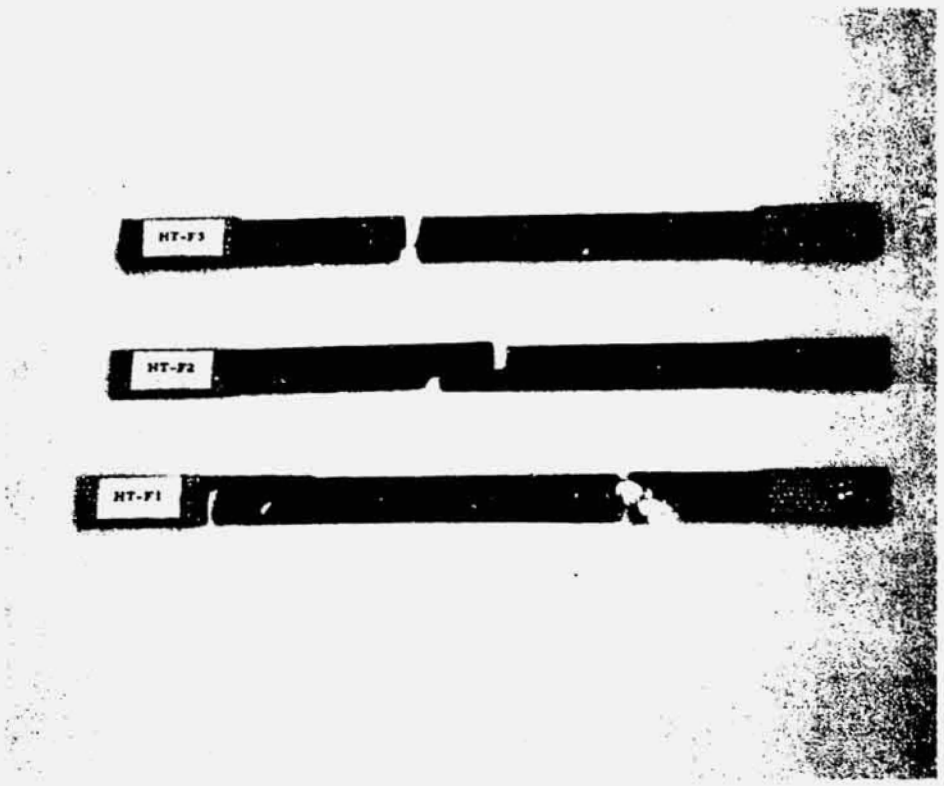

V_f	σ_c x10^3psi	E, x10^6psi
.31	56.5	12.1
.51	63.8	19.6
.56	138.0	21.6

a) HT-U Fiber Specimens (Original Batch)

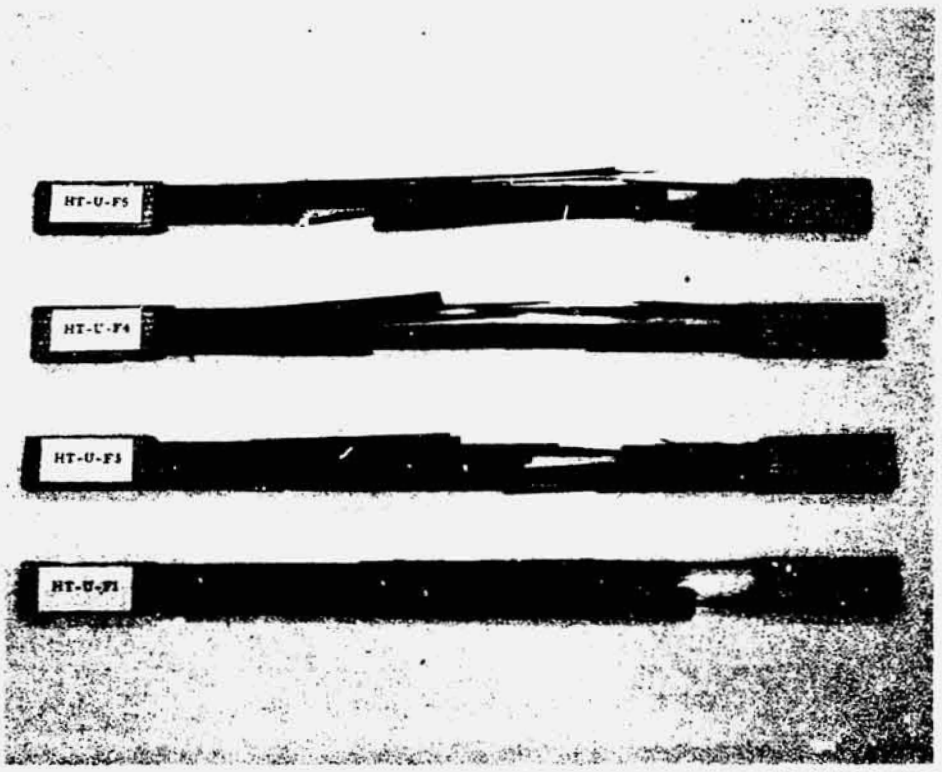

.45	143.0	17.8
.51	139.0	20.0
.63	130.0	25.0
.47	149.0	18.5

b) HT-U Fiber Specimens (New Batch PPH)

Figure 10. Comparison of Gross Failure Modes for Tensile Specimens of HT Fibers in Modified Resin

mechanisms would be introduced by surface treatment. This is indeed the case with the unmodified resin system, as shown in Figure 11. The upper photo shows how untreated fibers behave with typical fracture at a single location and no other fiber fractures along the axis of the specimen. Note that there is some evidence of fiber pullout on either side of the fracture with the untreated fibers (upper photo).

The lower photo shows the behavior of the treated HT fibers in the unmodified resin and, although the gross failure mode was the same (a single fracture site), there is no evidence of fiber pullout near the fracture and the fracture plane is almost perfectly planar compared to the upper photo. This indicates a very strong bond which results in nearly perfect cleavage as opposed to the more tortuous mixed fracture involving both interface failure and cleavage normal to the fibers. It should be noted that although both the treated and untreated HT fibers exhibit essentially the same gross response in this kind of very lightly reinforced specimen, the subtle differences at the interface may be more significant when a much higher volume fraction of fibers is present.

Figures 12 and 13 show a comparison of untreated and treated HT fibers in the modified resin formulation. In the upper photo of Figure 12 we see extensive debonding on the surface of the tow and no evidence of large cracks. Prior high magnification photos (Figure 6) have shown that although many fibers are fractured they are difficult to see because they have not cracked the matrix normal to the fibers but, instead, have separated from the matrix at the interface. When ultimate specimen failure did occur, a good deal of fiber pullout was observed for the untreated fibers (see lower photo of Figure 12).

Surface treated HT fibers behave quite differently in the modified resin as shown in Figure 13. Several cracks are apparent (middle photo), spaced at about 3 to 4 diameters along the tow. The upper photo shows one of these cracks at 60X with no obvious debonding. The regions of debonding at the left of this photo are probably due to some variations in fiber orientation since they do not appear on the right of the photo where the fibers seem to be very straight. Finally, the lower photo illustrates how one of these crack sites resulted eventually in fracture of the specimen. Only a few fibers have been pulled out and these are very short, indicating a good bond between matrix and fibers.

From these observations it appears that the surface treatment does result in a stronger bond between HT fibers and the epoxy novolac system in both the modified and unmodified formulation. Since the bond is sufficient to fracture the fibers in the untreated condition, one would expect no improvement in tensile strength by applying such a treatment to the fibers. Indeed, this seems to be the case if we examine manufacturer's data for tensile strength of treated and untreated fibers. The primary reason for the surface treatment is to improve the interlaminar shear strength and it has been demonstrated that a 30 to 50 percent improvement can be realized with the higher bond strength obtained with treated fibers.

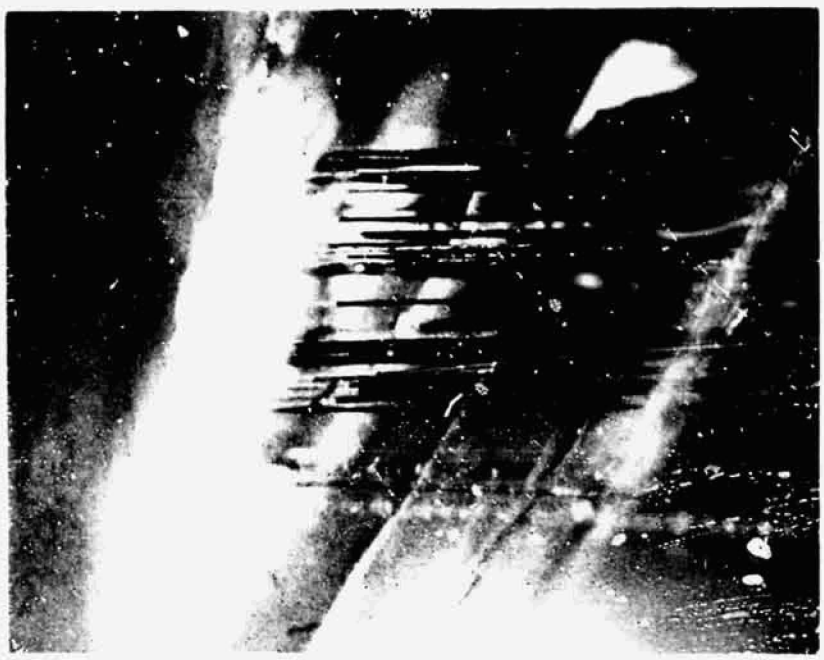

a) HT-Untreated Fibers - 60 X

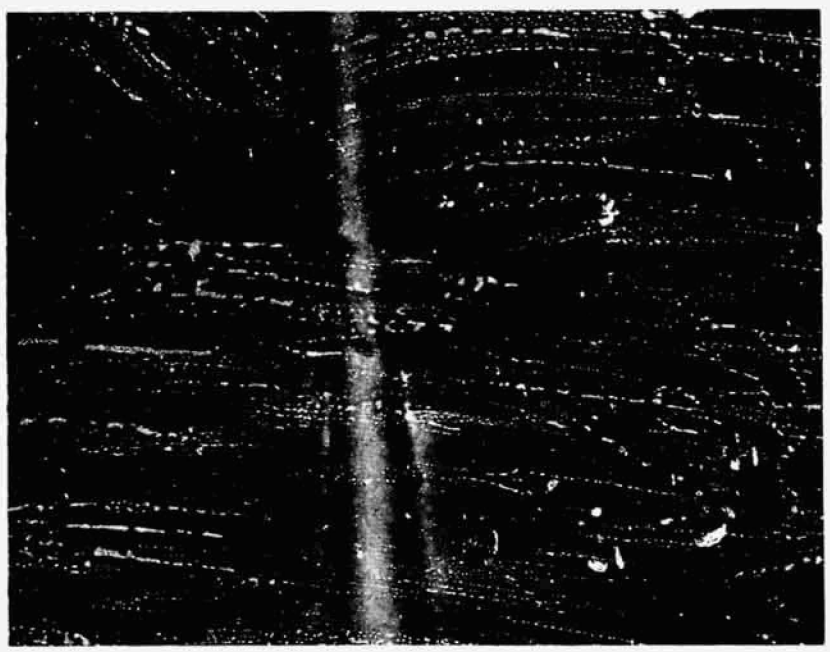

b) HT-Treated Fibers - 60 X

Figure 11. Comparison of Tensile Behavior of HT Fibers in Unmodified Resin

a) HT-Untreated Fibers 28 X
(New Batch)

b) HT-Untreated Fibers 60 X
(New Batch)

Figure 12. Tensile Behavior of Untreated HT Fibers in Modified Resin

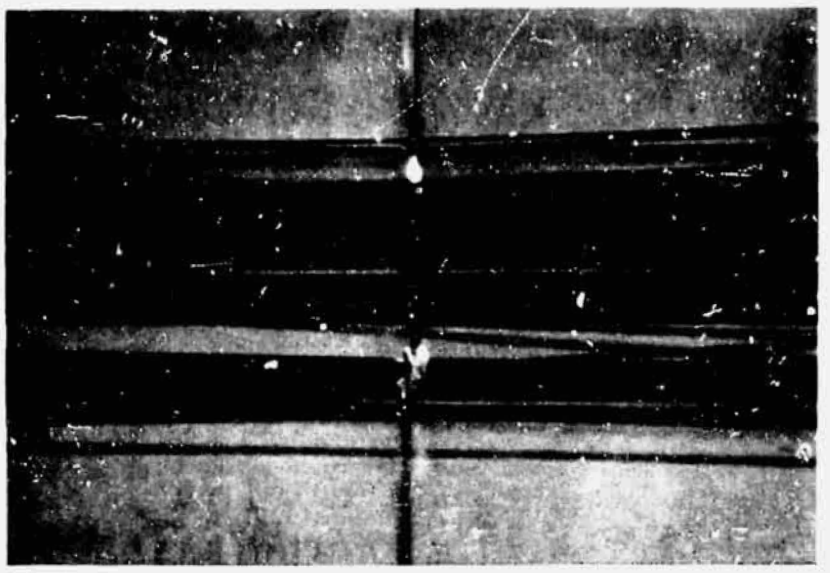

a) 90% of Ultimate Load
Disc Shaped Cracks @ 60 X

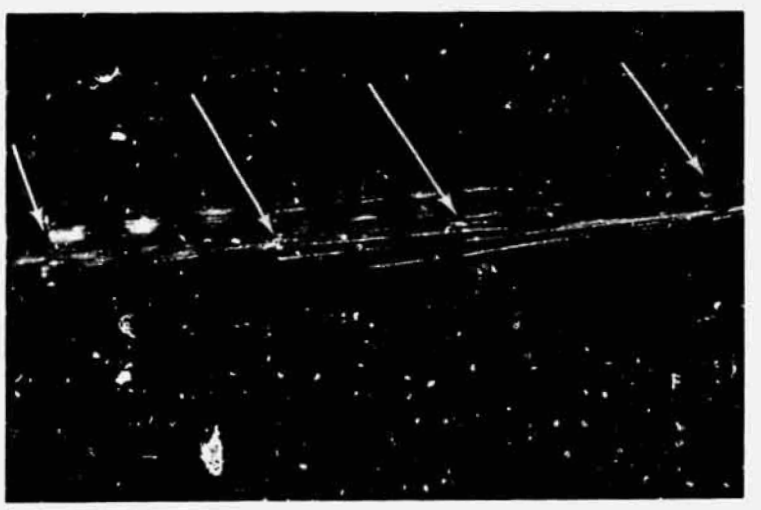

b) Debonding and Disk- Shaped
Cracks at Final Failure - 28 X

c) Final Failure Showing Fiber
Pullout - 60 X

Figure 13. Tensile Behavior of Treated HT Fibers in Modified Resin

3.2.2 SURFACE TREATED TYPE A FIBERS IN EPOXY

Figure 14 shows a comparison of untreated and surface treated Type A fibers in the unmodified resin system. Although there is some very slight evidence of fiber pullout in the upper photo, the fracture modes are essentially the same with the first fiber fracture resulting in specimen failure. No sign of cumulative damage was evident and this is consistent with previous observations in the unmodified resin system.

Figures 15 and 16 illustrate the behavior of untreated and treated Type A fibers in the modified resin system. The untreated fibers shown in Figure 15 have fractured at regular intervals along their length with very little matrix cracking at the fiber sites. The higher magnification lower photo shows how local debonding has occurred near the fiber fractures thus diminishing the energy available to generate matrix cracks normal to the fibers. Note also that only a few of the fiber fracture sites in the upper photo exhibit such cracks. This indicates a bond-limited failure process as had been observed with untreated Type A fibers in last year's work.

Figure 16 shows how treated type A fibers behave in the modified resin system and the results are rather interesting. The upper photo shows a collection of matrix cracks coalescing into a major fracture site. Note, however, that these are not disk-shaped high energy cracks as had been observed in all previous specimens but, instead resolved shear cracks which initiate at about 45° to the fiber axis forming the familiar "bow tie" pattern. This means the fiber fractures first without generating a sudden high energy (disk-shaped) crack. Then the high shear at the newly formed ends, instead of causing debonding (as with the untreated fibers in Figure 15), generates tensile cracks in the matrix on the planes where tensile stress is maximum (at 45° to the fiber axis). As these cracks grow further from the interface, the stress trajectories become more parallel to the fiber and thus the crack turns more or less normal to the stress trajectory (and fiber). From that point on the crack grows to a critical size and eventually the specimen fails. The interesting point here is that, by surface treating the Type A fibers, an interface limited system has been changed to a matrix (tension) limited system but without evidence of high energy cracking normal to the fibers. The significance of this change on bulk composite properties has not yet been determined but will be evaluated as the program progresses.

3.2.3 PRELIMINARY EXPERIMENTS WITH ERLA RESIN

Because of its higher heat distortion properties, the ERLA 4617 resin system has generated a a good deal of interest. Further, the system can be modified much the same as the DEN 438 system discussed previously. It was therefore selected for study and comparison with the DEN 438 system. The only comparison completed thus far with the ERLA 4617 formulation is the study of treated and untreated Type A fibers in single tow specimens.

Figures 17 and 18 show that surface treated fibers behave the same as untreated fibers in this resin. This is not surprising since the mechanical properties of ERLA 4617 are similar to those of unmodified epoxy, and the single catastrophic crack failure occurs in

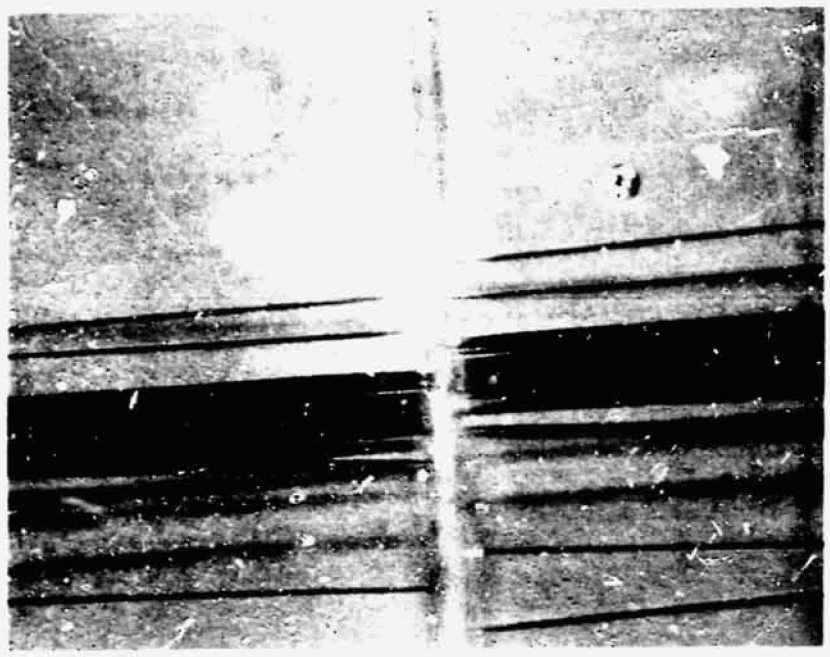

a) Type A-U (Untreated) Fibers - 60 X

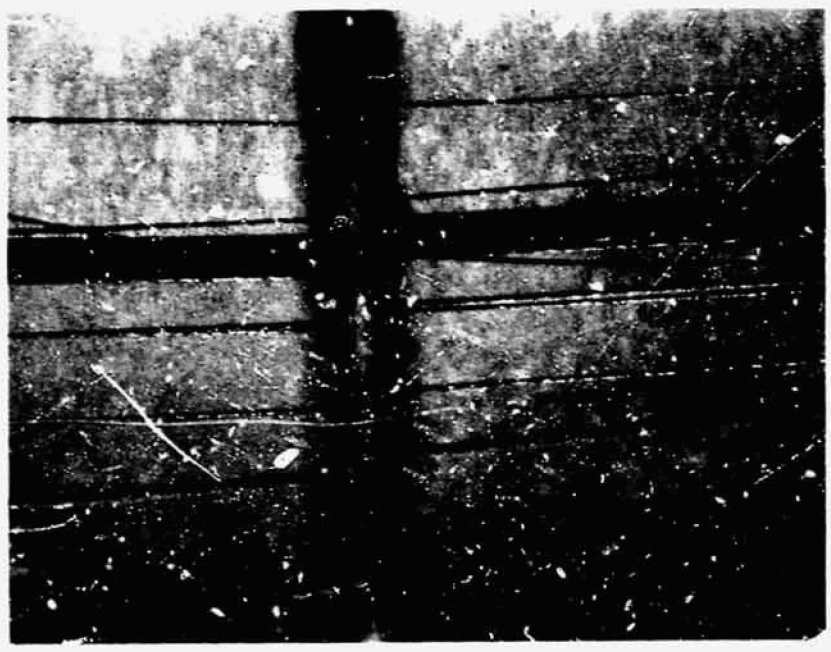

b) Type A-S (Treated) Fibers - 60 X

Figure 14. Comparison of Tensile Behavior of Treated and Untreated Type "A" Fibers in Unmodified Resin

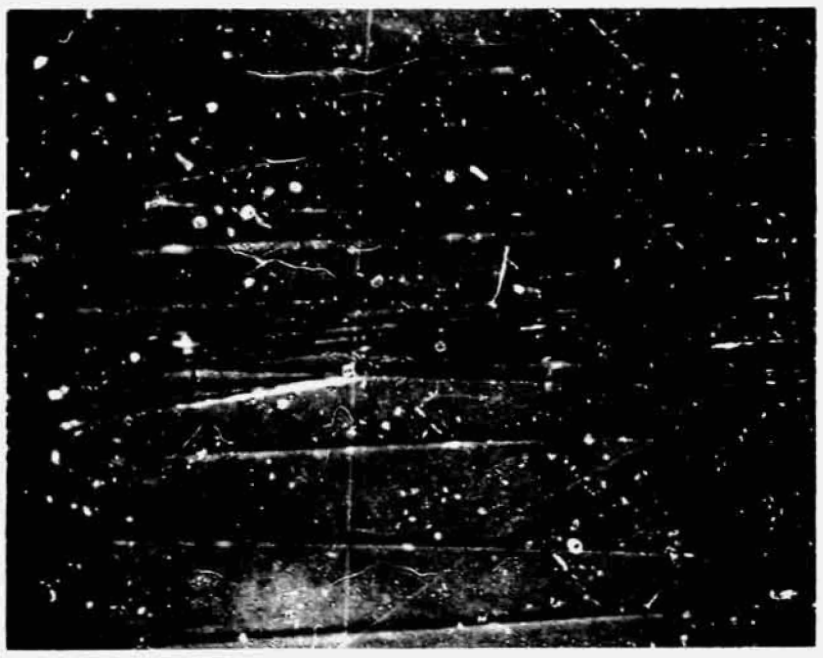

a) Type AU (Untreated) Fibers
60 X

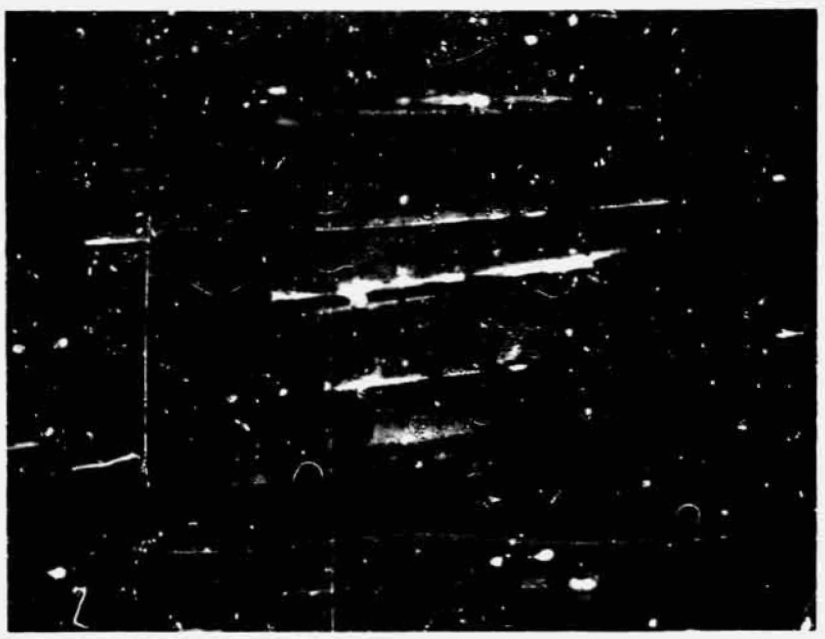

b) Type AU (Untreated) Fibers
150 X

Figure 15. Tensile Behavior of Untreated Type A Fibers in Modified Resin

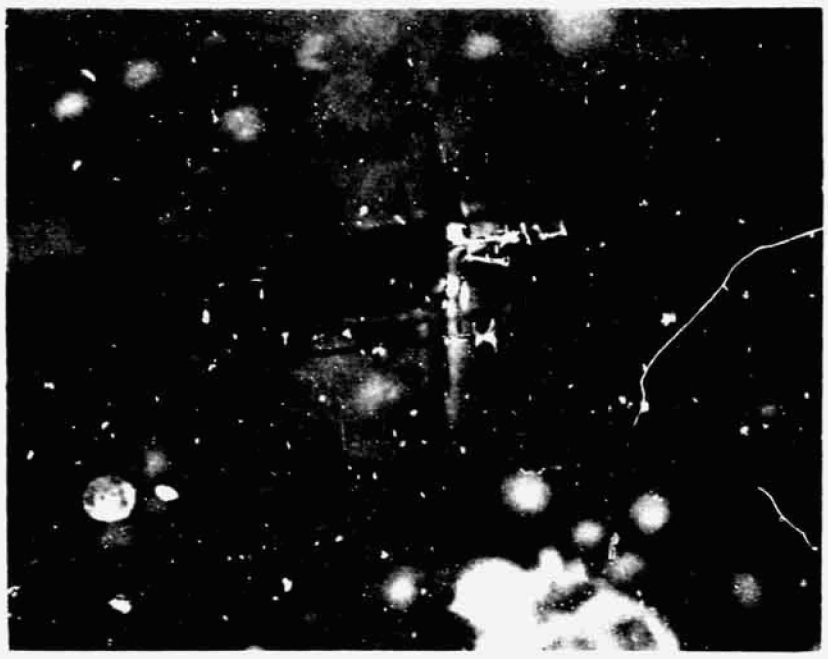

a) Type AS (Treated) Fibers
60 X

b) Type AS (Treated) Fibers
150 X

Figure 16. Tensile Behavior of Treated Type A Fibers in Modified Resin

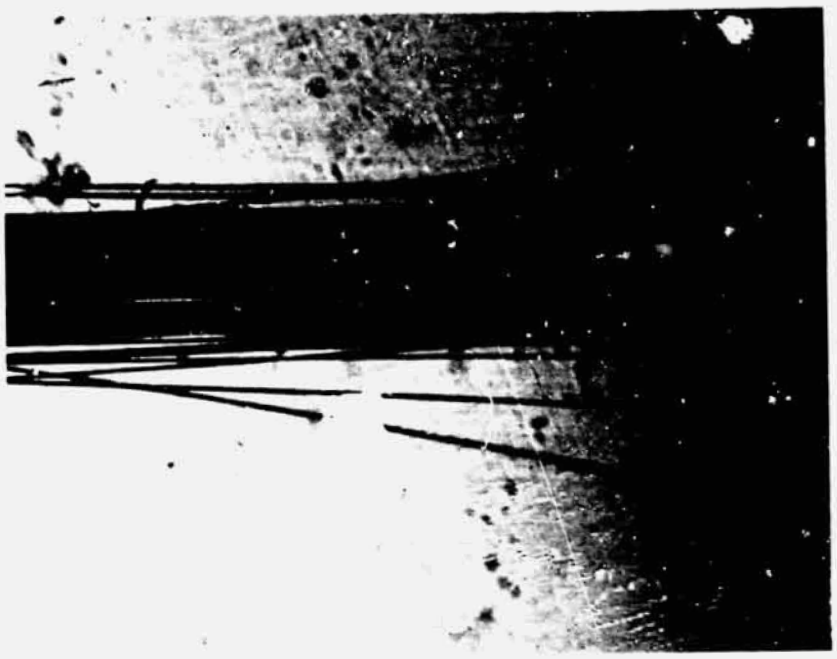

a) 70% Ultimate Load.
Type A Treated Fibers - 60 X

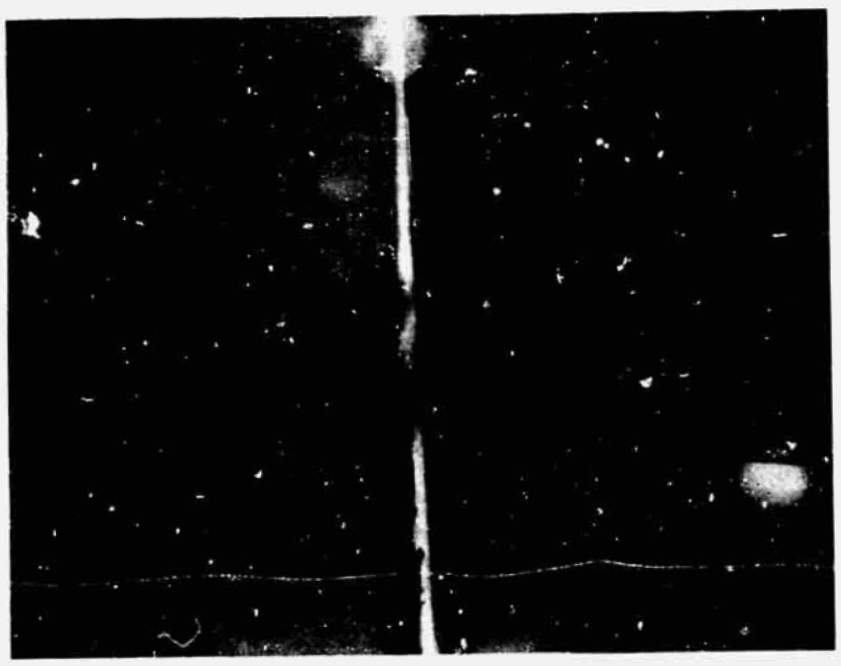

b) Final Failure - Type A
Treated Fibers - 60 X

F.gure 17. Tensile Behavior of Type A Treated Fibers in ERLA 4617 Resin

a) 90% Ultimate Load
Type A Untreated Fibers
60 X

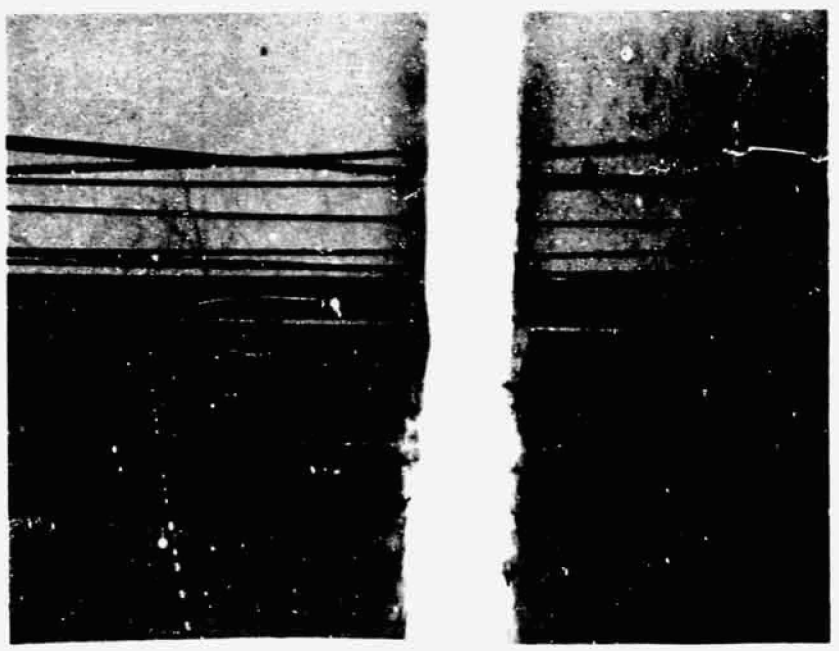

b) Final Failure
Type A Untreated Fibers
60 X

Figure 18. Tensile Behavior of Type A Untreated Fibers in ERLA 4617 Resin

both resin systems. There is no evidence of fiber pullout in either case and the fracture surface is quite clean, suggesting a very high energy failure progressing on a single plane. Specimens are now being prepared with the ERLB system containing both treated and untreated HT and Type A fibers.

3.3 ACOUSTIC EMISSION STUDIES

3.3.1 BACKGROUND

When metals, polymers, composites, or other materials are subjected to a load, local failure events such as slip, twinning, fiber fracture, etc., results in the sudden release of energy. The elastic wave is produced by this energy release is transmitted through the material and can be detected by suitable instrumentation. The study of such events, either by counting them or analyzing by other means, constitutes the area of acoustic emission. The first systematic work in this area was performed by Kaiser in 1950 [8], and further fundamental work has been conducted by Schofield [9], Liptai [10], and Tatro [11].

Acoustic emission techniques have been in use in the Space Sciences Laboratory for about two years, and the primary emphasis has been placed on the analysis of the failure modes in composite materials and ceramics. The equipment is illustrated in Figure 19 (with the exception of the counting device which will be described later), and a block diagram of the instrumentation is given in Figure 20. The transducer used in all cases has been an Endevco Model 2226 accelerometer. The acoustic data is stored on an Ampex tape recorder operating at 15 ips, which allows frequencies up to about 80 kHz to be recorded. An oscilloscope is used to monitor both the input and output signals. Depending on how the data is to be treated, output read-out devices can be a spectrum analyzer (for frequency analysis), a high speed oscillograph, or a counting and summation system for recording acoustic events.

Initial work on the analysis of failure mechanisms in composites involved the use of low volume fraction boron epoxy specimens, and an attempt was made to acoustically identify the failure modes previously isolated by Mullin, Berry, and Gatti [12]. These fundamental modes were filament fracture, matrix cracking, and filament debonding. For the case of single fibers of boron embedded in a transparent epoxy, it was possible to correlate the above failure modes with a characteristic acoustic signature, one of which (fiber fracture) is shown in Figure 21. Furthermore, as discussed by Mullin and Mehan [13], for the low volume fraction boron epoxy case there seemed to be an identifiable frequency associated with these events. These were quantitatively measured on a spectrum analyzer. Figure 22 illustrates the type of data that can be obtained from the analyzer, where the acoustic signature of a single filament break in a glass epoxy specimen is broken down into its various frequency components.

3.3.2 CARBON EPOXY SPECIMENS

3.3.2.1 Experimental Considerations

When carbon epoxy specimens were first tested in tension and their acoustic emission monitored, several facts immediately became evident. First, the amplitude of individual

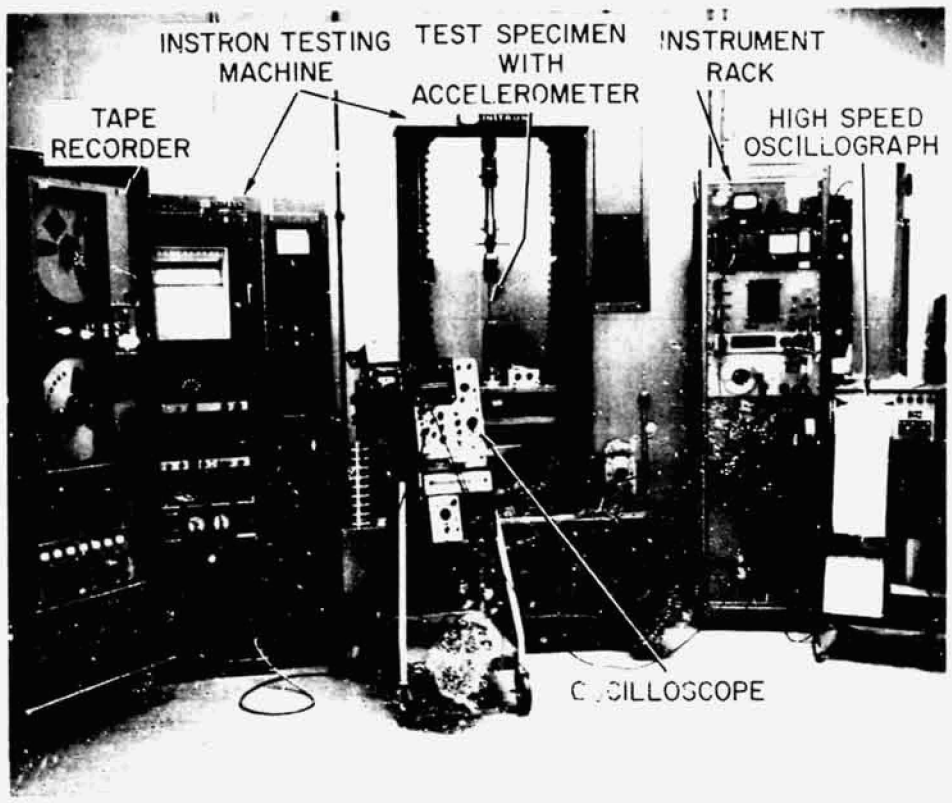

Figure 19. General View of Acoustic Emission Test Equipment and Associated Readout Devices

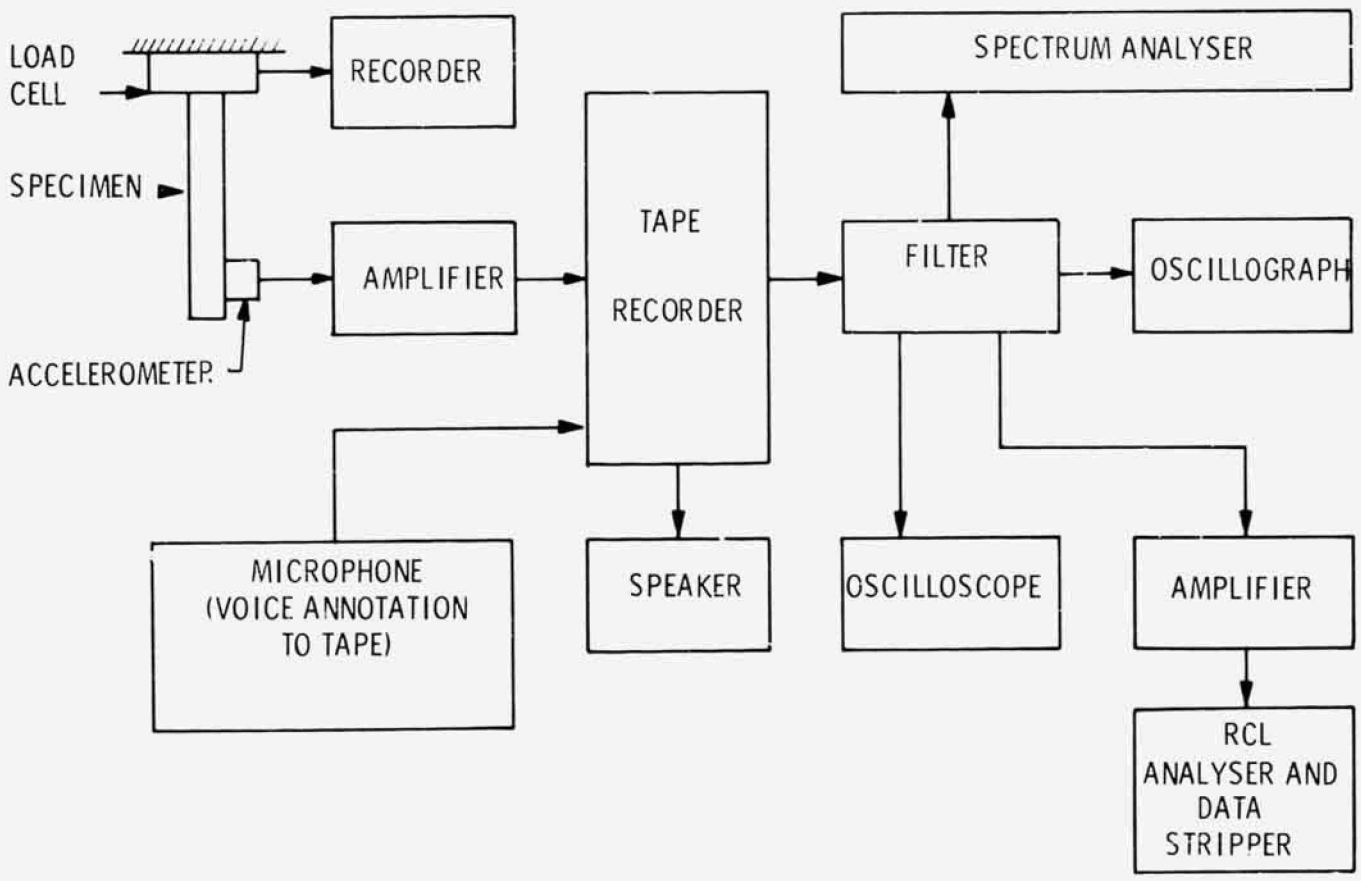

Figure 20. Schematic of Acoustic Emission Test Equipment

Filament and matrix fracture - 70x

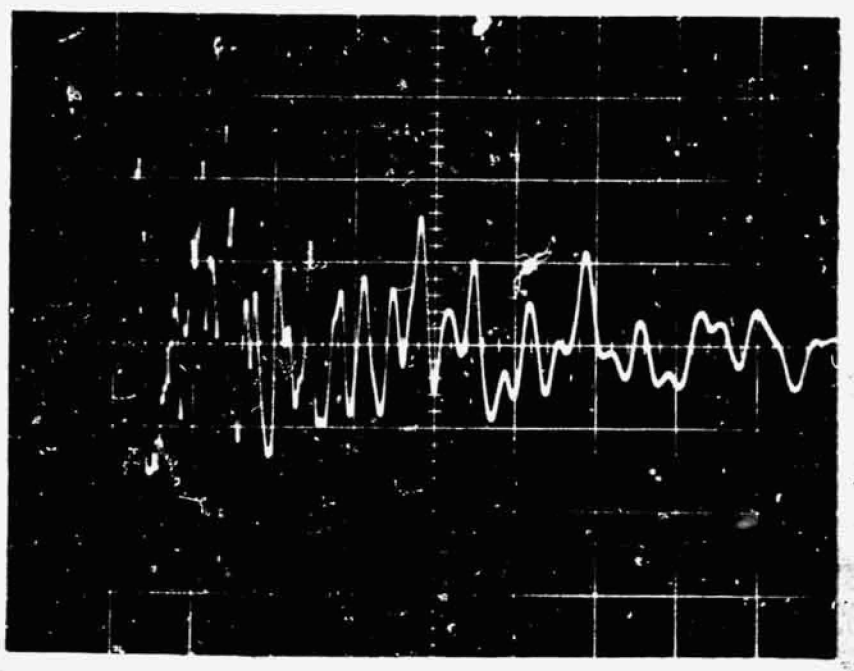

Oscilloscope record of fracture. Horizontal scale: 2 **msec/cm** **Vertical** scale: 0.1 volt/cm. 2x magnification during **recording**

Figure 21. Acoustic Signal of a Filament Fracture in a Single Filament Boron Epoxy Composite

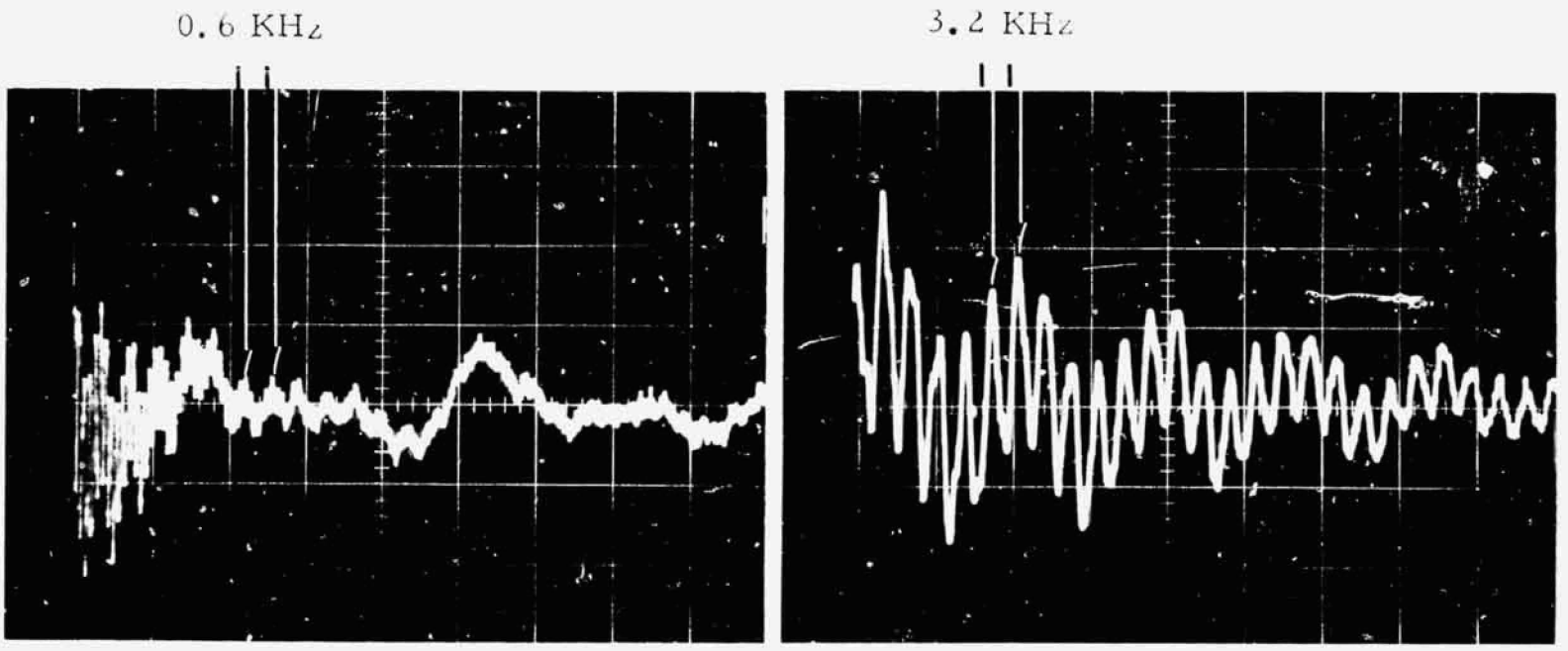

Horizontal Axis: 5 msec/cm

Horizontal Axis: 1.0 msec/cm

Signature of Acoustic Event

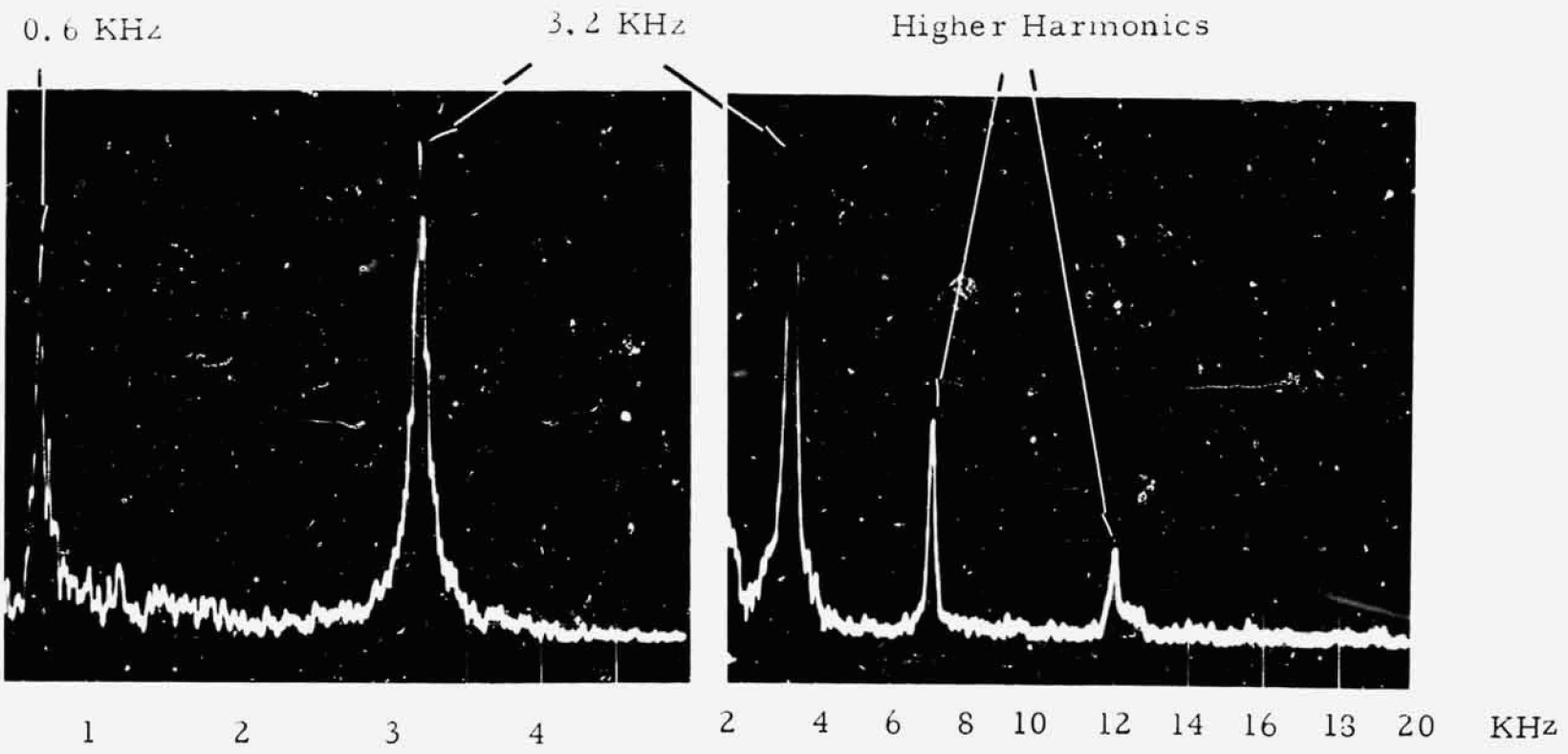

Spectrum of Acoustic Event. Note-Two Different Time Scales

Figure 22. Fracture of a Single Filament in a 70 v/o Glass-Epoxy Specimen During a Tension Test

events was much lower in the case of carbon epoxy specimens as contrasted to boron epoxy. For boron epoxy, an amplifier attenuation level of 20 dB was used, while for carbon epoxy 60 dB was necessary. Secondly, because of these low amplitudes, predominant transducer resonant frequencies of 48 kHz were observed. With boron epoxy, sufficient energy was available to excite lower frequency modes such as specimen vibration. Finally, the number of events was much greater than before. Because of these various factors, it became clear that, with these fibers, techniques involving counting the acoustic events should be utilized.

To perform this function, the apparatus shown in Figure 23 was utilized. On the top of the instrument rack is shown a Hammer amplifier employed to digitalize the data, as explained in more detail below. The lower instrument in the rack is a 400-channel RCL analyzer; capable of counting and storing data at the rate of 10^6 events/second per channel. The middle instrument is a digital data stripper, used to electronically integrate rate data to cumulative data. The top instrument is a display oscilloscope. To record the data, an X-Y recorder is used to transcribe the data from the analyzer memory bank.

Most acoustic emission instrumentation records several counts for an individual event such as a fiber fracture. This is illustrated in Figure 24. For small amplitude events, the transducer is set into resonance by the travelling elastic wave as described previously, and will produce the damped sinusoidal signal shown in Figure 24. The amplifier which converts the data to digital form has an adjustable discriminator level, below which the data is not counted. In the example shown in Figure 24, the discriminator level is set such that the particular acoustic event shown is "counted" three times. Obviously, higher energetic events will result in a higher count, as will events which physically occur in the specimen near the transducer as contrasted to those occurring at some distance from it. These factors must be kept in mind when analyzing count data obtained from a particular test.

When working at reasonably high gain levels (greater than, say, 50 dB), considerable care must be taken to prevent the introduction of spurious acoustic noise introduced by the gripping system. Metal-metal contact produces copious emissions under load, presumably because of the interaction of surface asperities. Similarly, wedge-type grips using serrated surfaces are unsuitable because the deformation introduced by them causes spurious acoustic signals. Finally, the adhesive bond between the end tabs and the specimen can produce acoustic signals as the bond line is deformed.

The factors detailed above were not important when working with boron-epoxy composites because of the relatively low gain used. However, when carbon epoxy composites were being evaluated, it was evident that a different load train and gripping system had to be used. Wedge grips were replaced with pin-loaded grips, and rubber coated pins were used to avoid metal-metal contact between the pin and metal end tabs. In addition, teflon tape was wrapped around all thread connections in order to further reduce metal-metal contact.

Experimentally, noise produced by the bond line and the deformation introduced by the pins bearing against the specimen and end tabs proved the most difficult to eliminate. Dunegan, et al., [14] have described a method of prestressing the pin area to eliminate extraneous

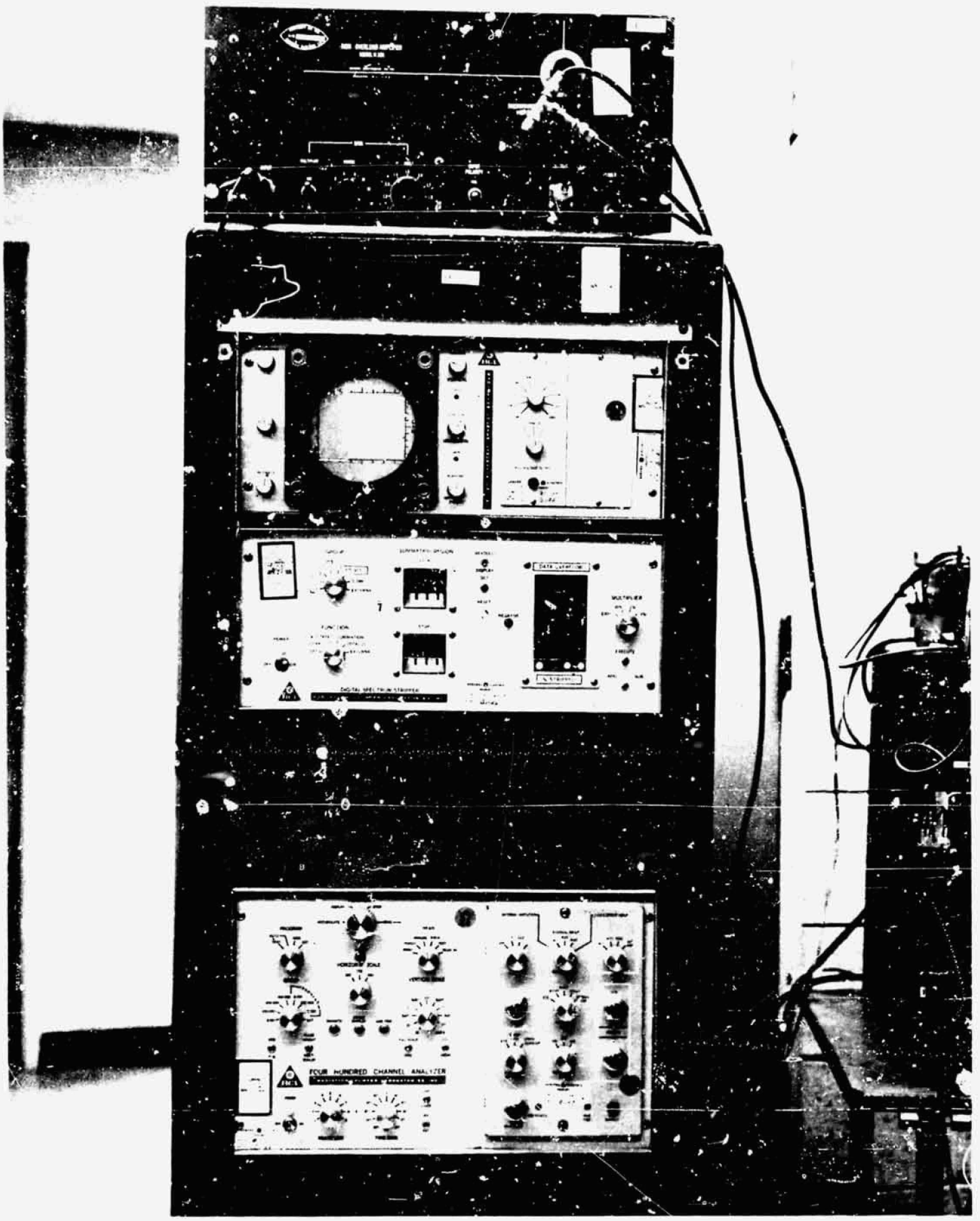

Figure 23. Photograph of Acoustic Emission
Event Counting Equipment

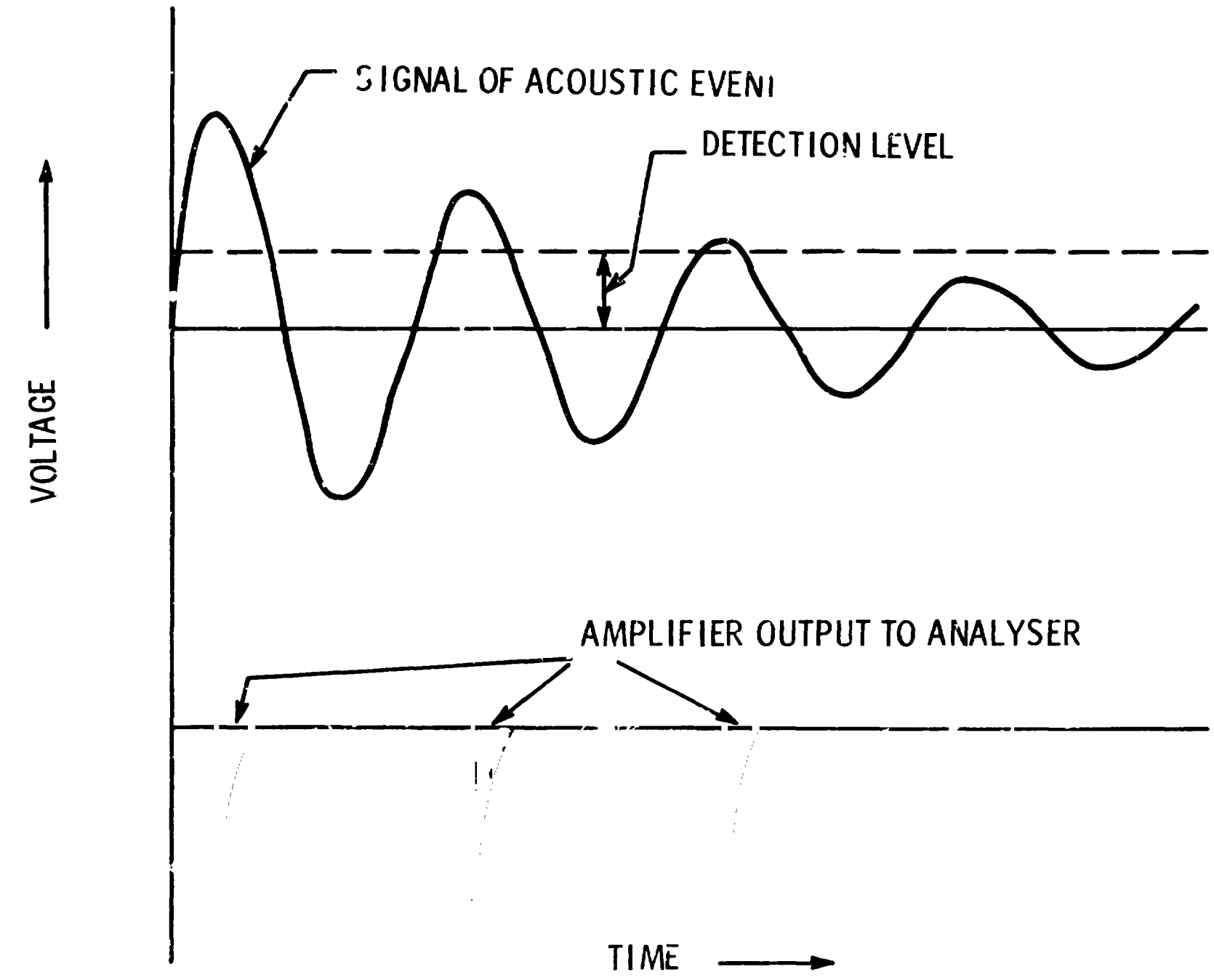

Figure 24. Schematic Illustrating Conversion of an Acoustic Event to Digital Form

noise in metal specimens, but this was found insufficient for the case of adhesively bonded end-tabs on composites. The procedure used in this investigation to check various experimental loading configurations was to load a steel specimen of the same size as the carbon epoxy composite with end tabs bonded in the same manner. At the attenuation level used (60 dB), steel did not produce acoustic emissions, so any noise recorded would be due to the loading method and end tab attachment used. Using this method, and the preload procedure described by Dunegan, et al [14], it was found that the bond still produced an unacceptably high noise level in the first loading cycle. Subsequent loading cycles eliminated these spurious signals, so the problem resolved itself into devising a method to load the bond line without loading the specimen.

The method finally adopted is shown schematically in Figure 25, and the assembly itself is shown in Figure 26. The area between the two loading pins was subjected to a preload, while at the same time the upper pin (used to hold the specimen during test) was firmly seated and the area around it preloaded. Although the area below the lower loading pin was not subjected to load until the specimen was actually tested, the number of emissions from this area (based on the steel "calibration" specimen previously described) were not large and could be ignored.

A specimen after preloading and prior to tensile testing is shown in Figure 27 with the accelerometer bonded to it. The reduced gage length was 3 inches long and 0.175 inches wide, and the filet had a 4-inch radius. The end tabs were 2-1/2 inches long. The entire specimen was 9 inches long, 1/2 inch wide, and about 1/16 inch thick and was made by the procedure described earlier in this report.

The experimental techniques used to load the specimen have been described in some detail because of the importance of this subject. Properly designed and acoustically quiet loading methods are absolutely imperative if valid acoustic emission data is to be obtained.

3.3.2.2 Micro Failure Mechanisms

As discussed previously in this report, when a carbon epoxy specimen is deformed in tension, one of several failure processes may occur. A fiber break can be associated with subsequent debonding, which can occur in incremental steps, or the break can lead to the formation of a matrix crack. All of these events will produce an elastic wave capable of exciting the accelerometer at its natural frequency of about 48 kHz. In addition, more highly energetic events such as groups of fiber fractures or gross matrix cracking can, in addition to transducer resonance, excite lower frequency components such as specimen vibration. At the present time with carbon fiber composites, we are unable to discriminate between these various failure modes, and the resulting count rate data includes all failure modes. It is hoped that subsequent work may allow the identification. by frequency, of different failure modes. To date, all work has been performed on high volume fraction composites.

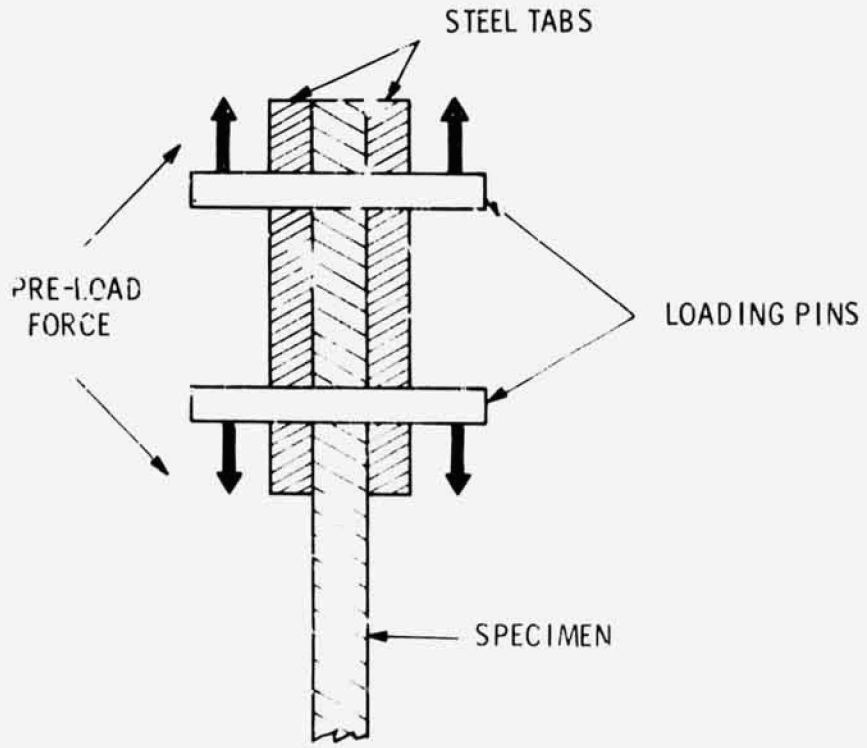

Figure 25. Schematic of Pre-Loading Fixture

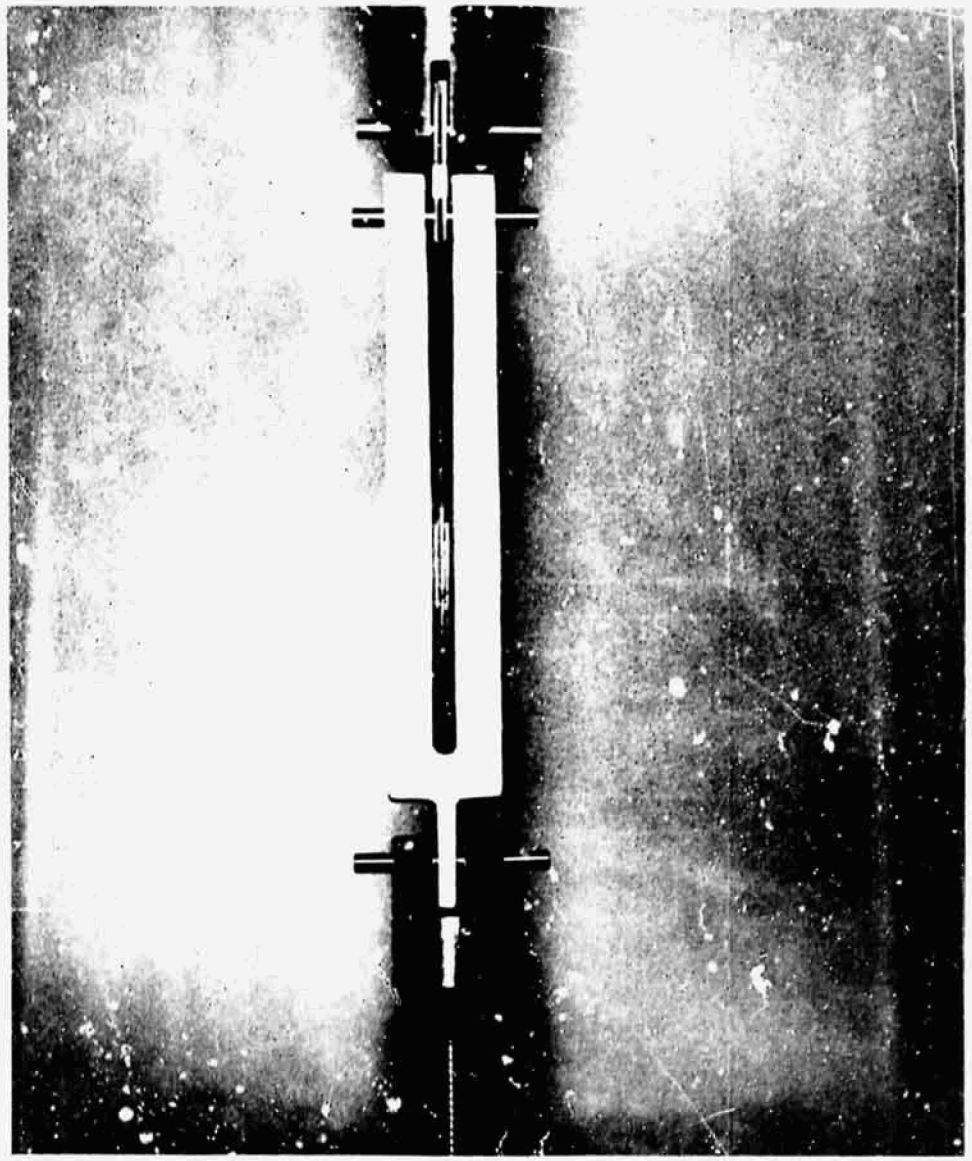

Figure 26. Photograph of Pre-Loading Fixture

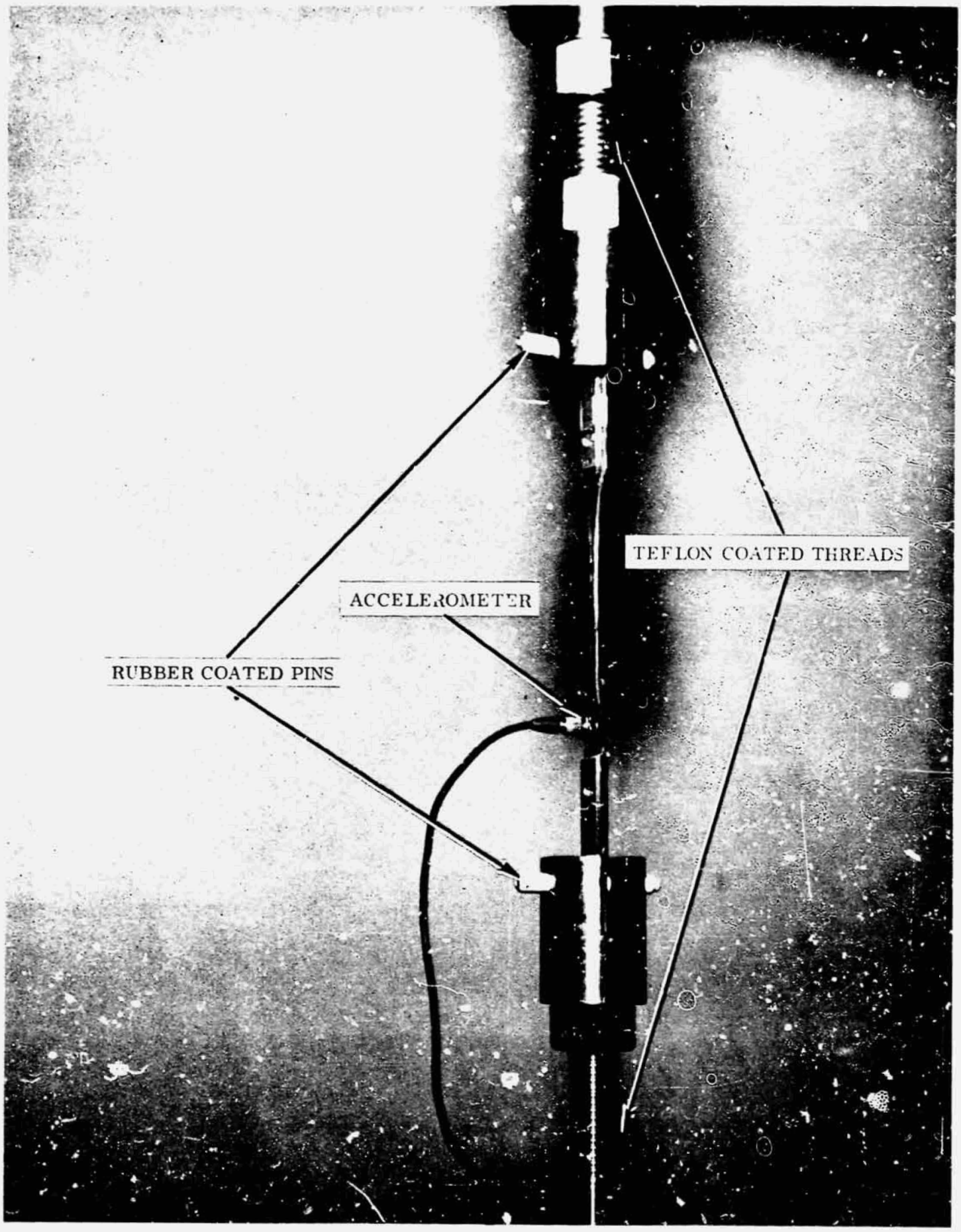

Figure 27. Photograph of a Test Specimen Ready for Test

A general idea of the frequency of occurrence of events may be obtained from Figure 28. Once failure events begin, they occur at an increasing rate. From time to time a burst of emission is noted, as shown in the top righthand photograph. This could indicate a larger group of fibers failing in close sequence, perhaps in conjunction with incremental de debonding. A typical individual event, consisting of an elastic wave exciting the transducer, is shown in the lower photograph. It may be noted that each event would be "counted" a number of times, depending on the discriminator threshold and the amplitude of the event.

Data showing the count rate and cumulative counts of acoustic events from three types of specimen are shown in Figures 29, 30 and 31. Figures 29 and 30 show the behavior of Type A fibers in both a modified and unmodified matrix, and Figure 31 shows the acoustic emissions emanating from a tension test of a composite consisting of HT fibers in an unmodified matrix. From these figures several conclusions may be drawn:

1. The acoustic emissions from specimens consisting of Type A fibers in either a modified or unmodified matrix are roughly the same. To a first approximation, this implies that the failure mode is similar in both matrices. When it is remembered that in no case was cumulative damage ever noted in single fiber specimens with any fibers imbedded into unmodified matrix (the first crack resulted in immediate failure) [15], it is clear that the presence of a number of adjacent fibers prevents such behavior. However, the acoustic emission data is consistent with the observation made last year [15] where the substitution of a modified for an unmodified matrix for high volume fraction composites containing Type A fibers did not result in appreciable strength change. The implication here is that high volume fraction specimens behave differently from single fiber specimens with matrix cracks being retarded by adjacent fibers at low to intermediate load levels regardless of matrix crack sensitivity. Of course, it must be remembered that the acoustic emission can equally well be caused by fiber fracture and subsequent debonding because the resultant elastic disturbances will excite the transducer in the same fashion. However, it is probable that the total energy emitted from a debonding failure would be lower than a fiber fracture, and hence result in a lower total number of counts. Because the count rate and total number of counts are similar in Figures 29 and 30, it seems likely that the failure mechanism is similar.

2. For the case of Type A fibers in an epoxy matrix (modified or unmodified), local failure events begin to be observed about half way through the test. This is not inconsistent with a statistical variation of fiber strengths and cumulative damage as discussed by Zweben [16].

3. By contrast, with HT fibers in an unmodified matrix (Figure 31), indications of failure begin earlier, and consist of isolated large amplitude events, the total number of events being less than obtained with Type A fibers in either resin. Assuming these earlier events are not spurious in nature due to grip deformation*,

*The data represented in Figures 29, 30 and 31 are based on only single specimens, and additional tests on duplicate specimens will have to be performed before complete reliance can be placed on the data.

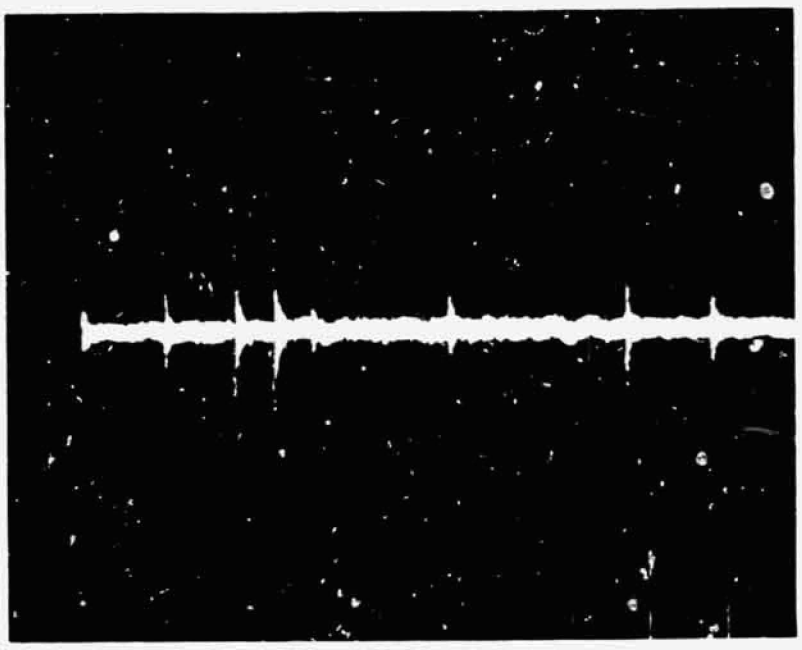

40 msec/cm
Average Emission Rate

40 msec/cm
"Burst" Emission Rate

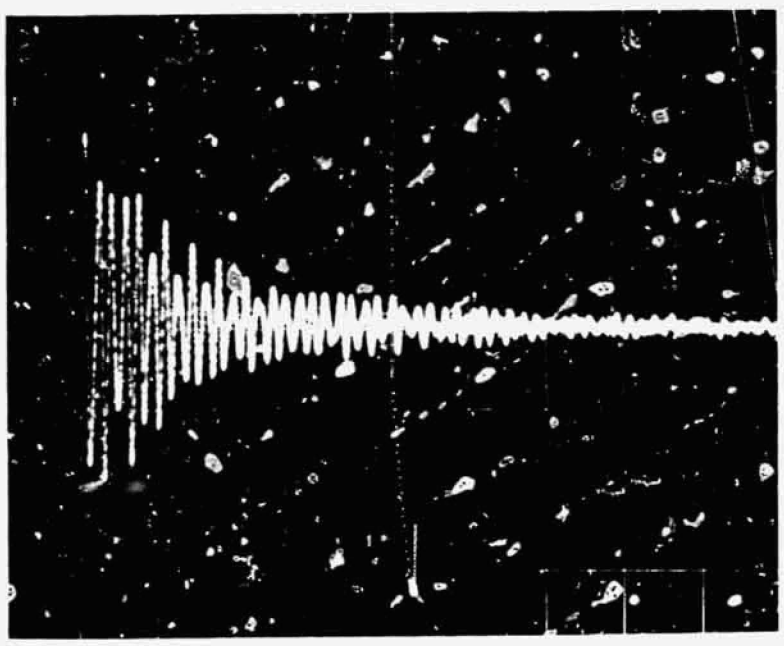

0.125 msec/cm
Typical Acoustic Event

Figure 28. Typical Emissions from a Carbon-Epoxy Specimen Consisting of A-Type Fibers in a Modified Matrix

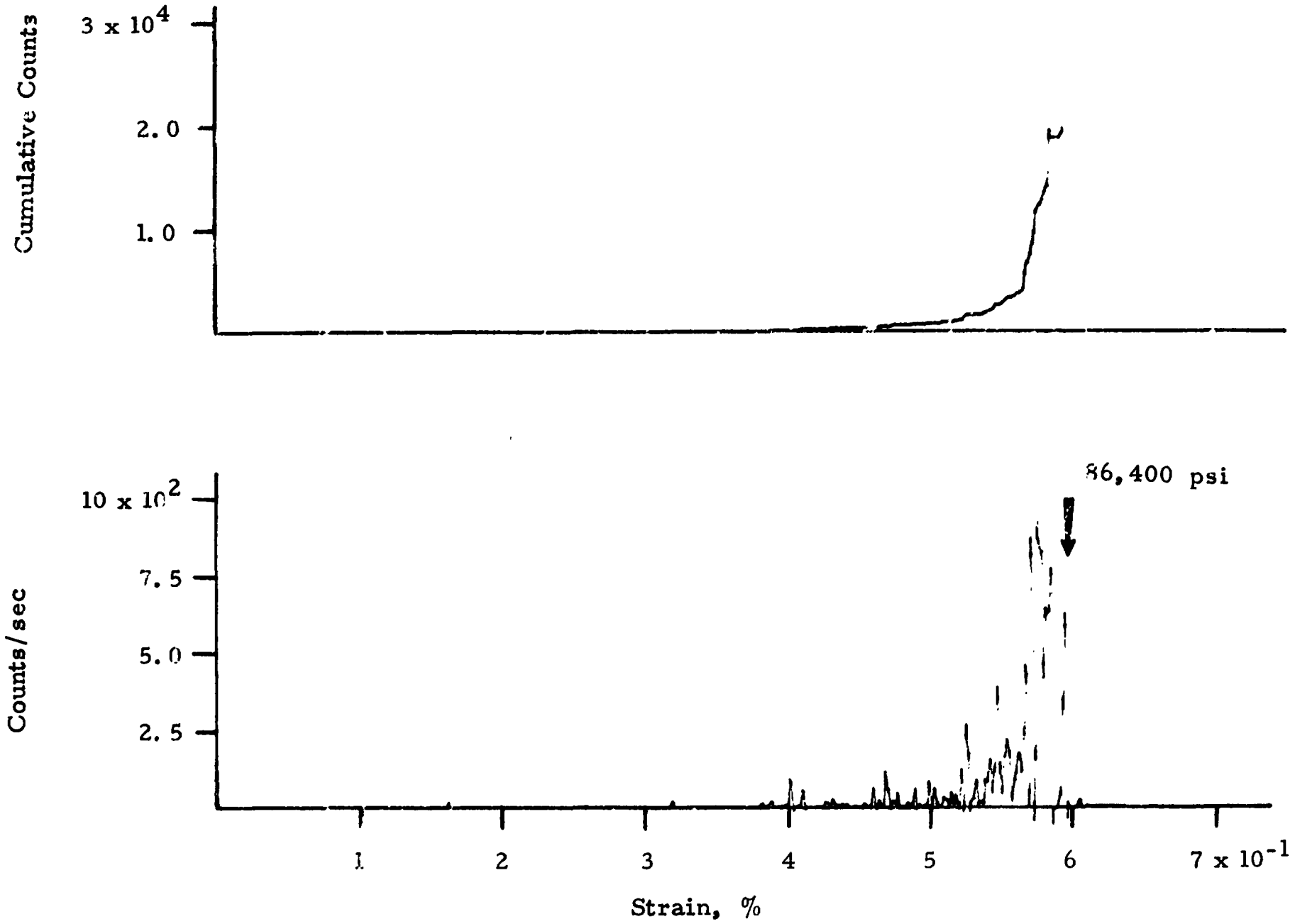

Figure 29. Acoustic Emission Test Data for a Carbon-Epoxy Specimen Consisting of A-Type Fibers in an Unmodified Matrix

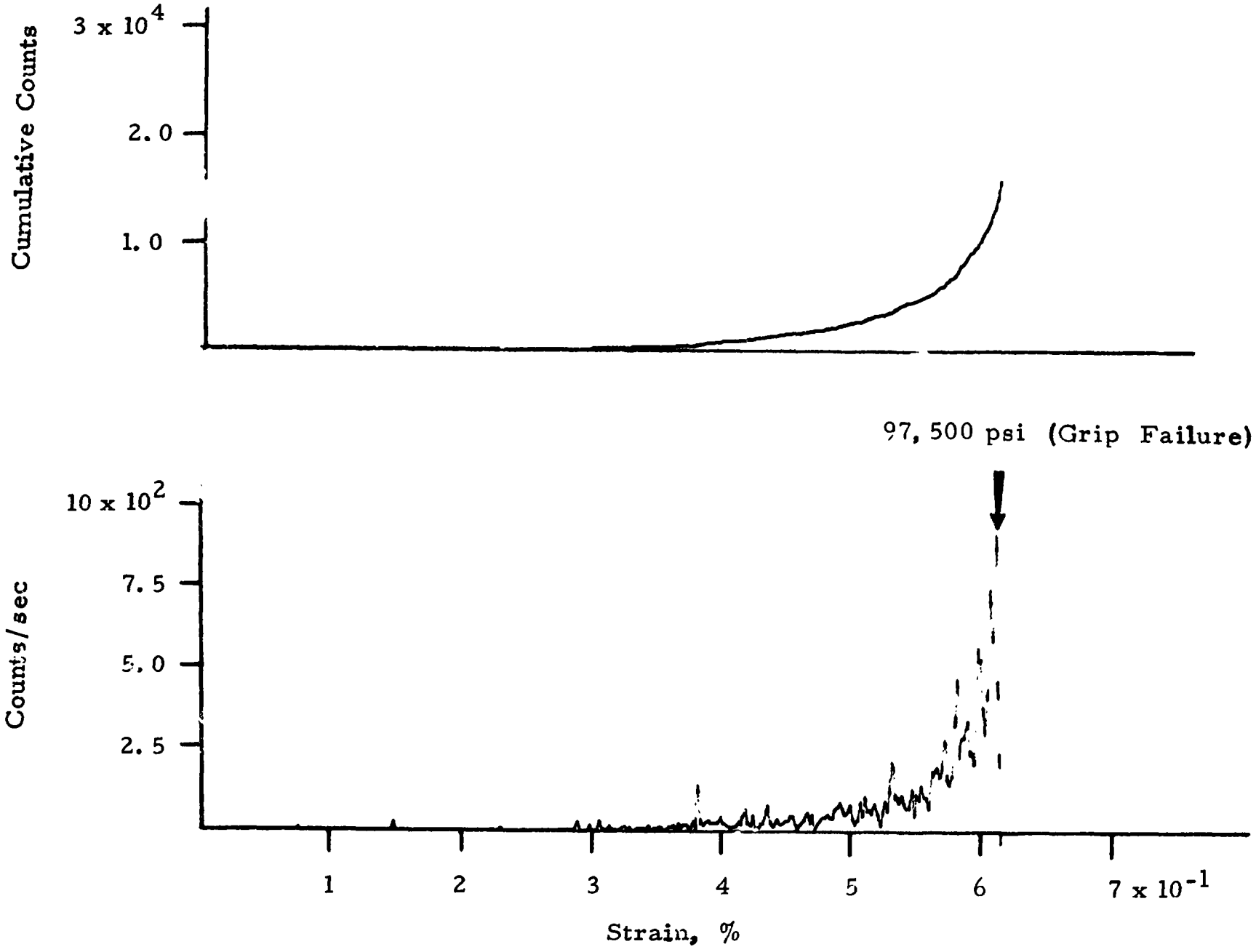

Figure 30. Acoustic Emission Test Data for a Carbon-Epoxy Specimen Consisting of A-Type Fibers in a Modified Matrix

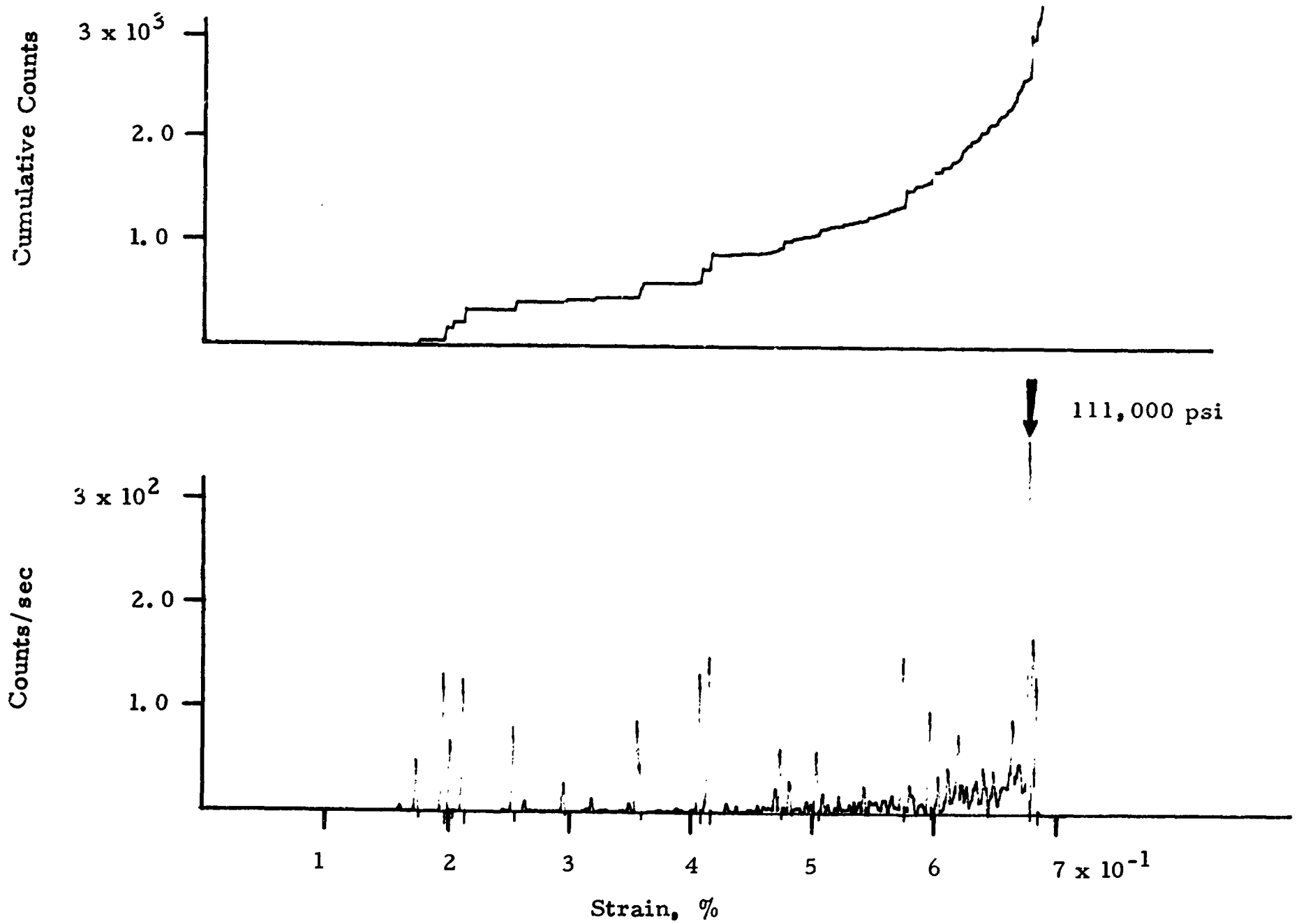

Figure 31. Acoustic Emission Test Data for a Carbon-Epoxy Specimen Consisting of HT Fibers in an Unmodified Matrix

it would seem that either large groups of fibers begin breaking early in the loading process or matrix cracking begins early. In addition, it may be seen that the rate of fiber fracture starting at about 4% strain increases less rapidly and does not reach as high a level as in the case of the Type A fibers. In fact, the test record depicted in Figure 31 can be considered to consist of the gradually increasing accumulation of fiber fractures (less than for the Type A fibers), with periodic large amplitude events superimposed. At the present time, the significance of these observations is not completely understood. The lower number of events observed for the case of HT fibers could be due to a smaller scatter in fiber strength. Conversely, if debonding does not occur to as great an extent in the HT case, and debonding gives rise to acoustic emissions, this could account for the smaller number of signals obtained as compared to the case of Type A fibers. These and other possible mechanisms will be evaluated for the remainder of the contract period.

3.3.2.3 Macro Failure Mechanisms

In addition to the failure events occurring on a fine scale and at relatively low amplitudes discussed in the previous section, larger and far more energetic events are observed as carbon epoxy specimens are tensile tested. These events are sometimes audible, and typically are recorded at an amplifier attenuation of about 20 dB. The origin of these events is thought to be both surface and sub-surface large scale longitudinal matrix cracking. Figure 32 shows such a failure, together with its acoustic signature. The specimen was unloaded prior to failure and the crack decorated with chalk dust to show greater contrast in the photograph. In some cases, similar acoustic events were observed, but no cracks were found, indicating that these failures can occur below the surface of the specimen.

The total accumulation of these failures is not large, perhaps consisting of a half dozen events during the test prior to failure. However, near the point of final failure, these large scale and audible events occurred with greater frequency. This is illustrated in Figure 33. Twelve seconds before final failure seven relatively large scale cracks occurred, and then the specimen failed in a catastrophic manner*. The moment of failure is represented in the bottom middle photograph, and the transducer was blown off the specimen. No detailed knowledge of the precise nature of the instant of failure is possible, because the intense degree of energy release sent a sufficiently large signal to the amplifier to saturate it. After failure, the transducer was not in contact with the specimen and any signal was due to the accelerometer striking the testing machine. After failure, as discussed in Section 3.1.2, the specimen was badly splintered. This is again illustrated in Figure 34, where several longitudinal matrix cracks were observed prior to failure and the specimen was unloaded and photographed.

*At the same time, of course, the rate of fiber fracture and other fine scale damage was increasing rapidly, as shown in Figure 31.

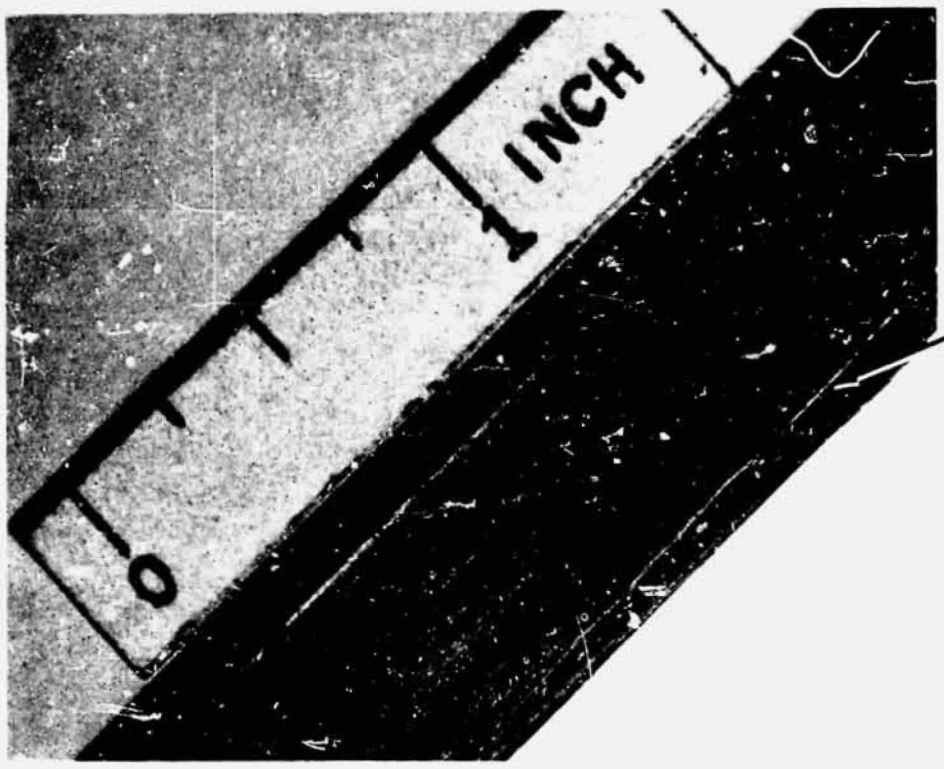

Unloaded Prior to Failure.

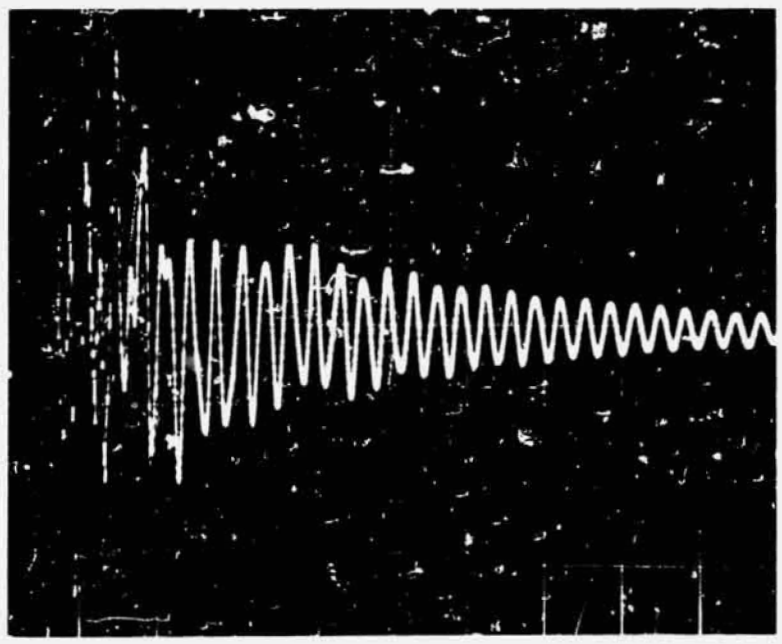

Acoustic Signature of Delamination

Figure 32. Photograph of a Longitudinal Crack in a Carbon-Epoxy Specimen and the Associated Acoustic Signature

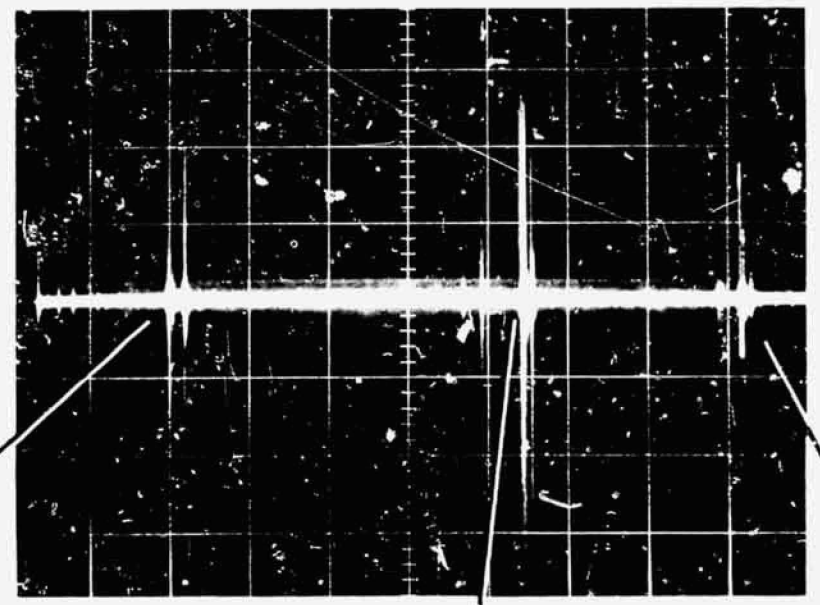

2 sec/cm

0.5 volts/cm

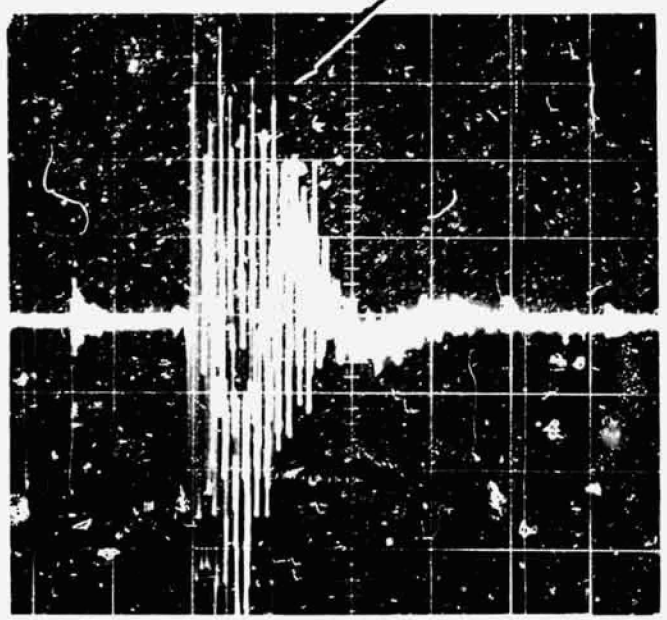

Precursor to Failure

2 msec/cm

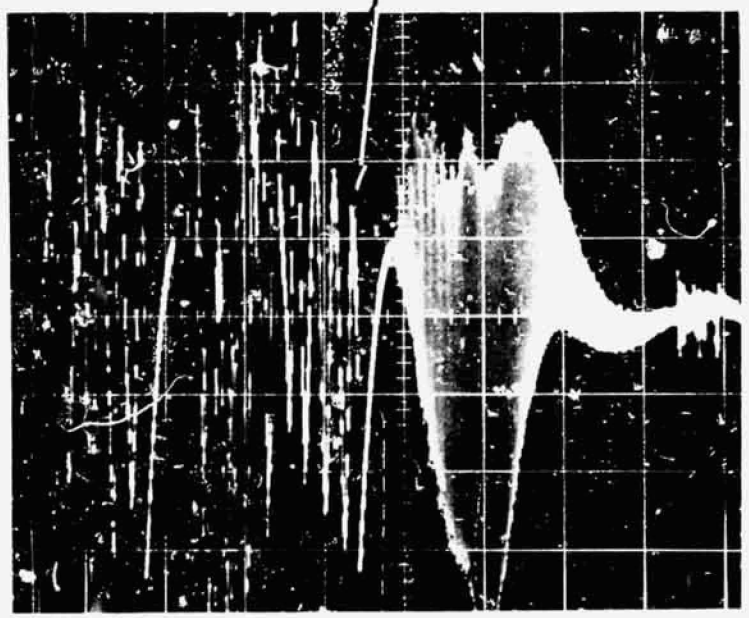

Moment of Failure

2 msec/cm

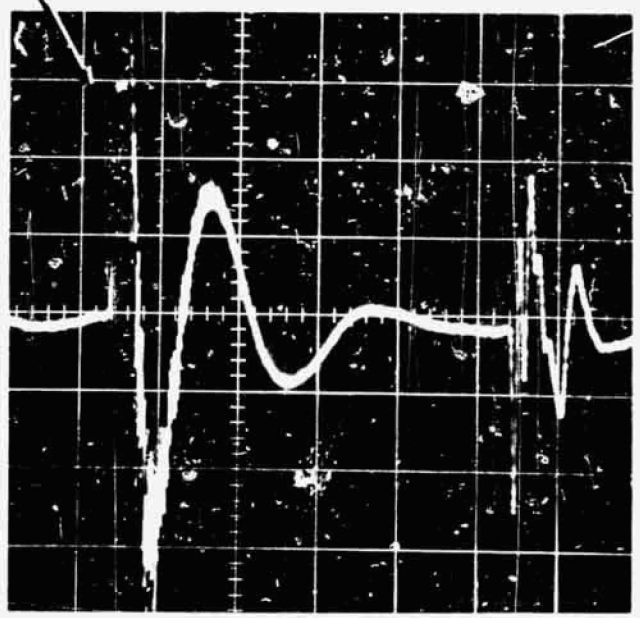

Signal Due to Transducer Hitting Test Machine

2 msec/cm

Figure 33. Acoustic Signatures of the Failure Process in a Carbon-Epoxy Specimen Consisting of HT Fibers in an Unmodified Matrix

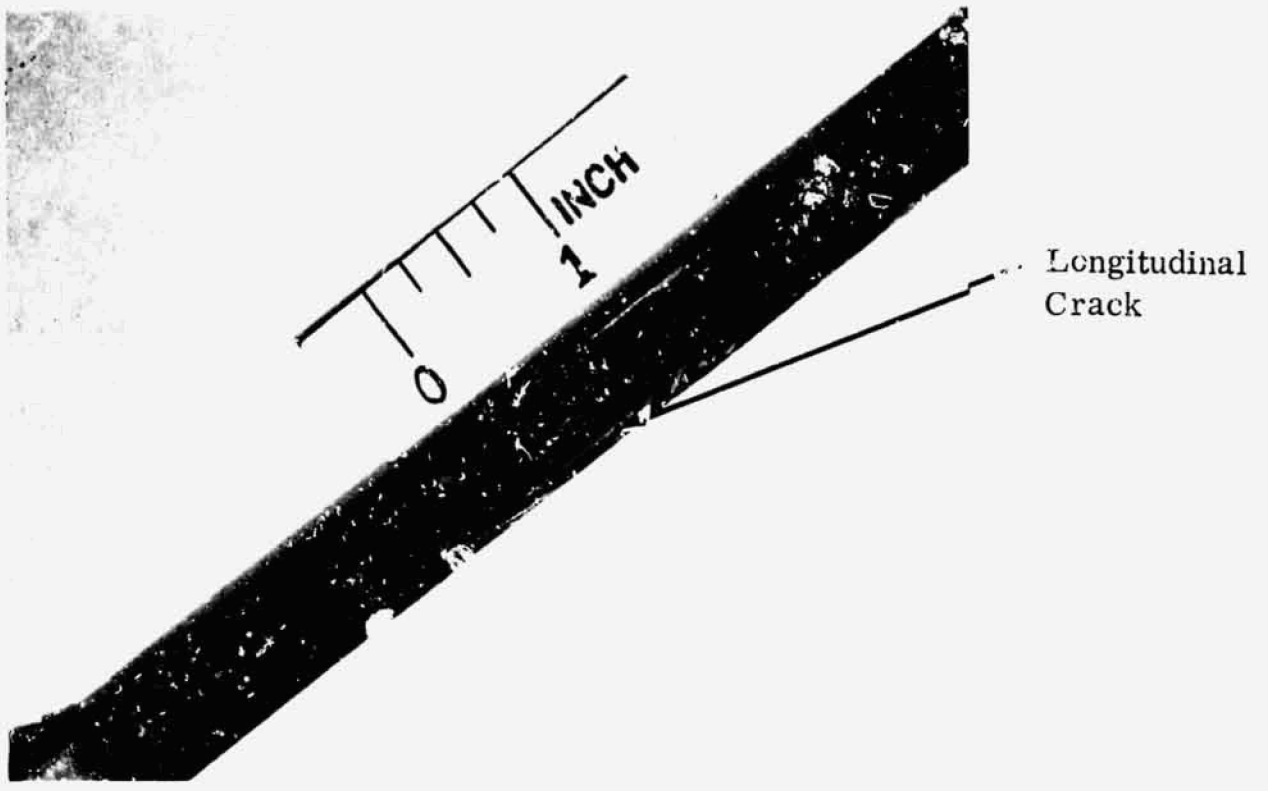

Unloaded Just Prior to Failure.

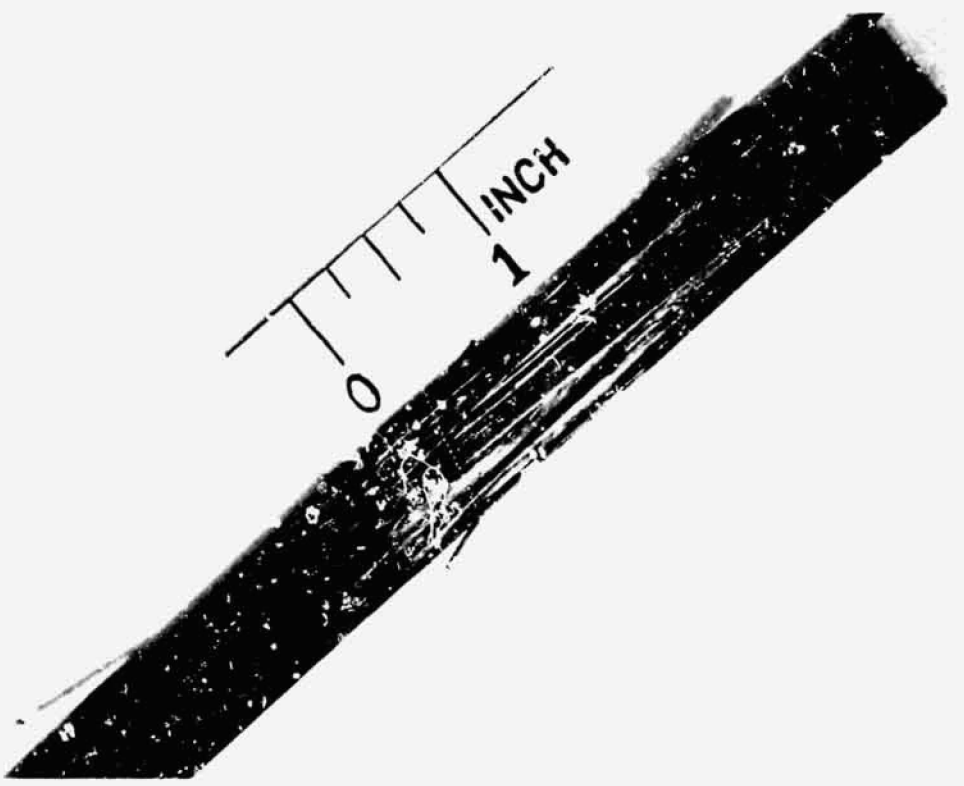

After Failure.

Figure 34. Photograph Before and After Failure of a Carbon-Epoxy Specimen Consisting of HT Fibers in an Unmodified Matrix

Based on the above observations, the following failure process is not unreasonable for tensile failure in a uniaxial carbon epoxy composite. Starting at about 50% of the failure load, fibers begin to fail and the rate increases with increasing load. Near groups of failed fibers, the matrix transmits the load between groups of fibers by shear. At intervals, the matrix shear stress is large enough to cause a local matrix crack, which can then propagate longitudinally some distance along the specimen length. This process continues until the longitudinal cracks link up by transverse cracks, and the specimen fails. The post-fracture shock wave, in the case where sufficient energy is available, then causes extensive splintering. This hypothetical reconstruction of the failure process needs more experimental justification, and this will be part of the effort during the remainder of this contract.

3.4 COMPOSITE/METAL SPECIMEN PREPARATION

In addition to the analysis of failure processes in composites there is a great deal of interest now in composites combined with metals as a result of initial efforts generated by NASA-Langley. Those efforts were focused on boron-epoxy tape bonded uniaxially to aluminum tubes in an effort to improve column strength. This approach offers great advantages for truss and strut applications since the boron-epoxy greatly increases the stiffness and strength while the aluminum provides an efficient means for making connections. Certainly the bond between the composite and metal is a critical link in this approach and the failure process can be limited by either of the two constituents or the interface between them. For this reason a thorough analysis of the basic failure mechanisms which occur in these composite-metal elements will be necessary to optimize their performance. The following sections outline some of the fundamental considerations in fabricating and characterizing these specimens relative to potential failure mechanisms. Both flat and tube-type specimens have been prepared and characterized to assure uniformity in the fabrication process. No test data is presented in this report since this phase of the program has just begun and insufficient data is available for analysis and discussion.

3.4.1 FLAT SPECIMENS PREPARATION

The effects of thermal mismatch between fibers and matrix, composite and adhesive, adhesive and metal substrate are dependent on both specimen configuration and fiber orientation. The problem is greater with carbon fiber composites because of the nearly zero thermal expansion coefficient in the fiber direction. To minimize distortions which can result from thermal mismatch in flat specimens, alternate layers of composite and metal must be used with symmetry through the thickness.

The two approaches taken in the preparation of composite/metal flat specimens were: first, to prepare the complete specimen in one operation using the matrix resin to bond to the metal; secondly, to cure the carbon/epoxy composite separately and bond it to the metal adherends after cure.

In the first approach there is the problem of obtaining sufficient resin at the bond line between the prepreg and the metal. Low prepreg resin content in such an approach can result in discontinuities in the bond line or the formation of voids near the bond line in the composite. In either case, a weakened region is formed which is likely to fail under the high shear stresses which develop on cooling back to room temperature. Although this approach is difficult, it is precisely the kind of process used in some hardware fabrication processes for composite/metal parts. For this reason it was considered important to evaluate in terms of failure mechanisms.

The second approach - fabricating the composite and then bonding to the metal - requires more time and is limited to certain configurations but provides better control of the bonding process. There are several advantages to this approach. First, better control of resin flow was possible when the composite material was cured alone. The cure cycle was less likely to impair the properties of the resin because the composite was first cured alone, and the resin not required to perform a dual function as in the first approach. Because lower temperature cures can be used with certain adhesives and the choice of adhesives is less constrained there is much less danger of introducing fabrication stresses. In some cases a room temperature curing adhesive can be used which has better chance of survival at cryogenic temperatures.

Briefly, the procedure used for preparing flat composite/metal specimens is as follows:

1. Lay up the required number of layers of preparing 0.5 inch wide x 9 inch long in the mold. Place the male section of the mold into the cavity.

2. Cure in a press for two hours at 350^{o}F; cool slowly to room temperature.

3. Lightly sand both composite surfaces for better bonding. Degrease surfaces with solvent.

4. Prepare the two adherend metal surfaces by vapor-honing. Degrease surfaces with solvent.

5. Apply room temperature cure adhesive in a thin layer to both prepared composite and metal surfaces.

6. Assemble the composite/metal specimen in the bonding fixture and place under clamp pressure.

7. Allow to stand at room temperature for ~ 16 hours. Complete cure in an air circulating oven for 2 hours at 200^{o}F.

8. Allow a slow cooldown to room temperature.

Figure 35 shows tensile specimens prepared by this process. Note in the top specimen - edge view - the individual outside layers of 1/32 inch thick 2024 aluminum and the uniformity of the 1/16 inch thick layer of composite material in the center. The lower specimen simply shows a top view of the specimen surface width and grips. Tensile testing and acoustic analysis was started on some of these specimens but data is insufficient to draw any conclusions at this point.

3.4.2 TUBE COMPOSITE/METAL SPECIMEN PREPARATION

The preparation of tube specimens is essentially restricted to the curing in-situ approach described in the previous discussion of flat specimens. One major difference is the fact that the composite is not constrained on both surfaces in the tube specimens as it had been when sandwiched between two metal surfaces. Since the composite is external to the tube and the specimen is axisymmetric, this does not result in distortion and the composite is better able to accommodate to shrinkage during cure.

The following series of pictures shows the procedure followed in achieving a good bond and good fiber orientation in the composite. Figure 36a shows a comparison of adherend surface before and after liquid-honing. The upper tube in the photo has been liquid-honed as evidenced by the satin finish. The surface is later degreased with a hexane. After solvent cleaning, an epoxy resin is painted on the surface and staged to a highly tacky condition. Photo b shows as-wrapped unidirectionally oriented carbon-epoxy prepreg material, over the tube, before cure. Figure 37 a shows shrink tube being placed over the wrapped assembly before cure. Photo b shows the shrink tubing being separated from the cured composite after cure. Note the shrinkage that occurred in the shrink tubing where it extends past the right end of the tube. Finally, Figure 38 shows the finished carbon-epoxy/metal tube.

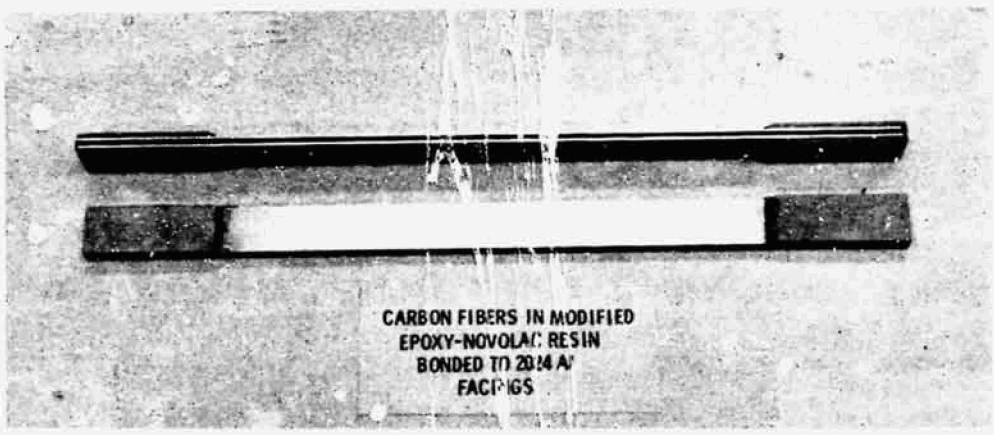

Figure 35. Typical Flat Carbon-Epoxy/Metal Tensile Specimens

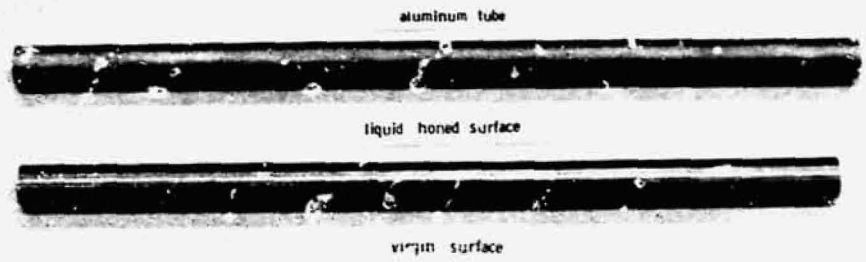

a) Comparison of Adherend Surfaces Before and After Liquid Honing

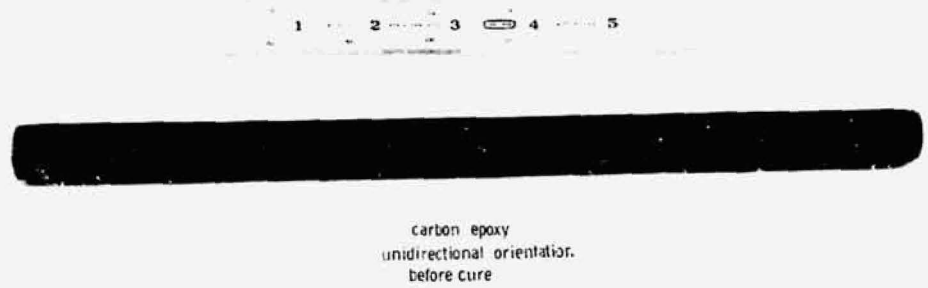

b) As-wrapped Unidirectionally Oriented Carbon-Epoxy Prepreg

Figure 36. Processing Carbon-Epoxy/Metal Tube Specimens-Steps 1 and 2

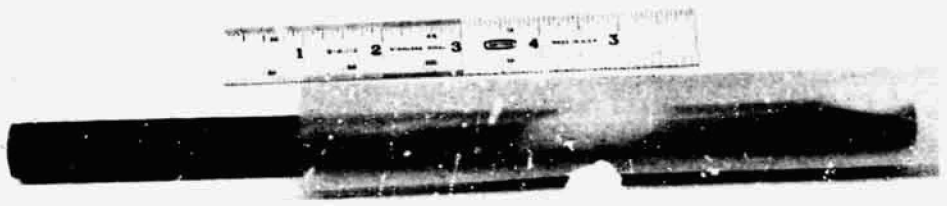

a) Shrink Tubing Being Placed Over Wrapped Prepreg Material Before Cure

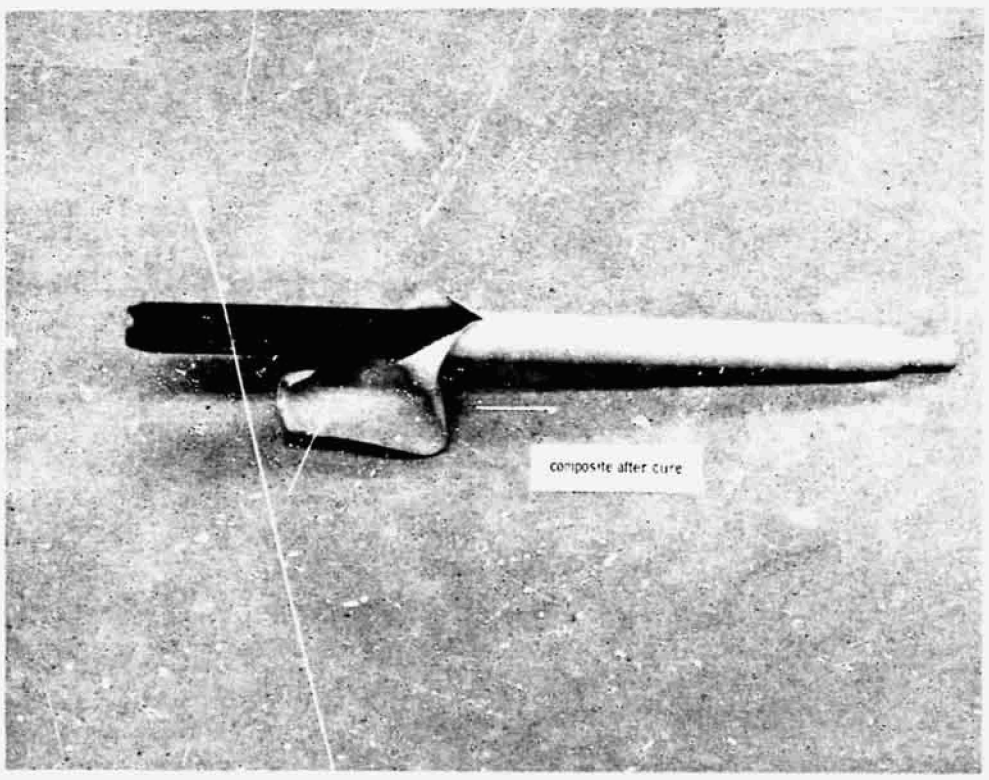

b) Shrink Tubing Being Removed After Cure

Figure 37. Processing Carbon-Epoxy/Metal Tube Specimens - Steps 3 and 4

finished carbon-epoxy-aluminum composite

Figure 38. Finished Carbon-Epoxy/Metal Tube - Ground, Machined and Polished

Final curing took place in an air circulating oven at 350° to 360°F for 4 hours, followed by a slow cooldown to room temperature. During the cooldown time the shrink tube remained in place over the specimen.

3.4.3 CHARACTERIZATION

The first step in characterizing the tube was to remove a one inch segment (Figure 39a) from the end section it, and examine the interface microscopically. Photos b and c show good bonding at the interface and also excellent fiber orientation in the composite at 60X magnification.

After microscopic examination, solvent was permitted to flow over the interface to further determine whether there was any debonding along the interface not visible under the microscope. Acetone was used in this test, and it evaporated uniformly along the complete interface length indicating no penetration into cracks. If minute cracks were present, evaporation would have been delayed at the crack sites.

End view examination, both visually and microscopically, indicated no delamination between plies, nor interfacial debonding around the periphery. Solvent wiping confirmed this also.

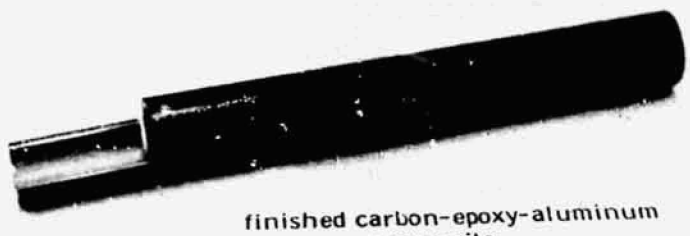

finished carbon-epoxy-aluminum composite

a) HT Carbon-Epoxy-Aluminum Tube

b) Cross Section of C/E/Al Tube 60X

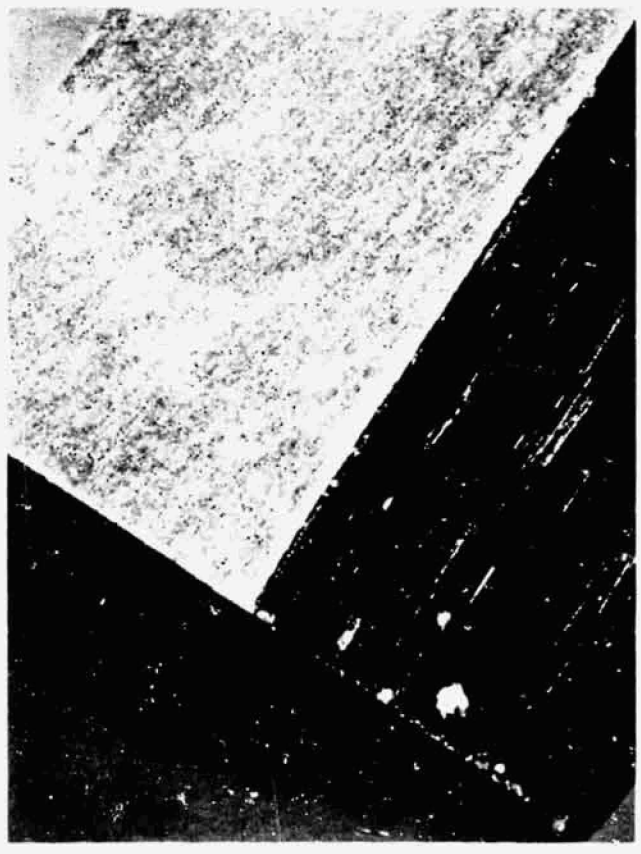

c) Edge of C/E/Al Tube 60 X

Figure 39. Composite/Metal Tube Showing Unidirectional Orientation of Fibers

From this preliminary evaluation, it appears that the technique is entirely satisfactory for producing good quality carbon-epoxy/metal tubes in short lengths. Tubes of greater length may require a different approach to compensate for the flexibility and bending during the material wrapping step.

Mechanical testing has not yet been performed on these tubes. The primary purpose of this preliminary effort was to develop a process for preparing good tubes.

3.5 FIBER COATING STUDIES (POLYURETHANE)

In the first year's work it was noted that failure mechanisms can be modified by coating fibers with either continuous or particulate materials. In that work it was found that metal coatings of silver and lead are effective in postponing failure for a period of time but do not allow gradual interfacial failure by debonding which is a far more stable failure mechanism.

Molybdenum disulfide particulate coating did not prevent the single fiber-break failure in the unmodified resin but did result in a more tortuous failure mechanism in the modified resin because of small tensile cracks near the interface.

Polyurethane coating was most effective in preventing catastrophic failure in single fiber specimens of unmodified resin. In every instance the polyurethane coating prevented the fiber from initiating specimen fracture which had never been possible for uncoated fibers. The polyurethane coating also allowed debonding and fiber fractures to occur before final failure. In every case the debonding progressed throughout the load history with the fibers breaking into uniform lengths until final fracture occurred. Although such a coating may reduce transverse tensile and interlaminar shear strengths, it shows great potential for preventing premature failure in tension parallel to the fibers.

During this year's study some work was done on developing a process for coating fibers and preparing tape for bulk specimens. This involved developing a dip process in which single tows and bundles were dipped by hand in a 13% solution in acetone. The coated fibers were allowed to air dry for 2 hours, followed by oven drying for 1 hour at 200^{o}F. Attempts were made at using lower percentages of polyurethane in acetone and other less volatile solvents, i.e., Isopropanol and xylene. It was found that a 4% polyurethane solution in acetone was best for uniform fiber coating. Isopropanol and xylene solvents were satisfactory, but coating on the fiber was not quite as uniform as with acetone. Microscopic examination of the fiber surfaces indicate a uniform coating and good fiber wetting.

The process for coating the fibers with polyurethane and preparing tapes with epoxy-novolac is as follows:

1. Lay short tows (about 12 inches long) of carbon fibers side by side on a thin Mylar film (5 tows to 1 inch wide).

2. Spray the tows with isopropanol to keep fibers straight and more easily workable.

3. Spread the tows open by rolling with a hard rubber or Teflon roller, being careful not to allow fibers to cross-over one another.

4. When tows are sufficiently laid open, remove excess alcohol and allow to stand until dry.

5. Spread each 1 inch wide strip onto a frame and clamp both ends securely.

6. Spray the strip with a 4% solution of polyurethane "Scotchcast" 221 in acetone until fibers are thoroughly saturated.

7. Allow to air dry for 2 hours at room temperature followed by oven dry for 1 hour at 200°F.

8. Light spray the 1 inch strip with low viscosity epoxy-novolac resin as a first pass to coat all fibers. Allow to air dry.

9. Heavy spray with a second application of epoxy-novolac. Allow to air dry until resin becomes slightly tacky.

10. "B" stage for 1 hour at 180° to 200°F in an air circulating oven.

Figure 40 shows a 1 inch wide by 5-1/2 inch long strip of prepreg material made by this process. The prepreg is approximately 12 mils thick which is about 4.5 mils thicker than commercially available prepregs. This is due to the fact that rolling was used instead of the pressure-squeeze roll technique used in commercial processes. Another problem was discovered during the preparation of a single tensile specimen made from the prepreg tape. It was observed after molding a 9 inch long by 5 inch wide by 0.062 inch thick specimen that the resin flash at the ends of the specimen were a little more porous than normal. After reviewing the process it was found that some of the solvent had been left in the polyurethane system and had formed voids during the final cure.

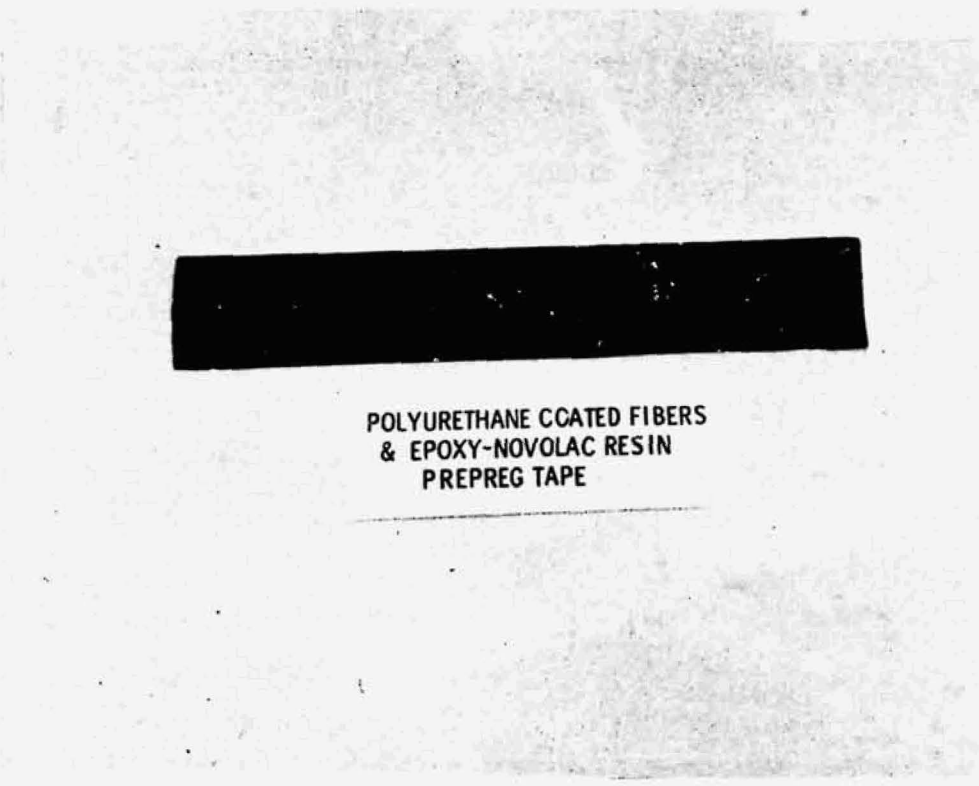

Figure 40. Carbon-Epoxy Prepreg Tape with Polyurethane Pre-coat

Since the primary purpose of the polyurethane coating was to enhance the performance of the original HT fibers so that higher composite strengths would result, the discovery that the new batch of HT fibers provided greater strength without coating diminished the importance of this effort. It was decided that before pushing ahead with the polyurethane coating approach it was essential to determine whether the newer HT fibers (both treated and untreated) were severely limited by cleavage as the original batch of fibers had been. Further, the effect of lower fiber volume fractions in the original batch bulk composite data had to be determined as discussed previously in this section.

SECTION 4

CONCLUSIONS AND PLAN FOR FUTURE WORK

Much has been done thus far to evaluate fundamental failure mechanisms for both HT and Type A carbon fibers in the treated and untreated condition. The ultimate goal is to identify the events which presage ultimate failure as a basis for improving composite performance. At the same time a thorough understanding of these failure events allows more reliable prediction of the response of composite structures under load. A vital link between these goals and the efforts described here is the use of acoustic analysis of the failure process in bulk composites once a cause and effect relationship has been established. Building on the progress made last year and the findings reported here, it may be possible to interrogate composite structural elements in service to evaluate their integrity.

The following specific conclusions can be drawn from the observations included in this report:

1. Two separate batches of untreated HT fibers have been found to exhibit different fundamental failure mechanisms in the same epoxy resin formulation. Although the differences in the unmodified resin formulation are subtle in single fiber specimens, the behavior is markedly different in the modified resin system. We conclude that either the strength of the original fibers has been degraded or there is a fundamental difference in the bond strength between the two batches of fibers. Fiber tensile tests are now being performed to resolve this question.

2. Bulk composite properties for the two batches of untreated HT fibers are also different with the newer fibers generally giving higher composite tensile strength for the same volume fraction of fibers. Manufacturer's data is essentially the same for each batch so we conclude that the differences observed in the single fiber specimens have very significant effect on bulk composite properties.

3. Observations of gross fracture modes in bulk composite specimens indicate that, for the same untreated fibers, cleavage fractures normal to the fibers are more likely to occur at fiber volume fractions on the order of 30% while predominantly longitudinal cracks are evident at fiber volume fraction on the order of 50%. This behavior suggests that because there is a larger sheath of resin surrounding each fiber in the lower volume fraction composites, there is more transfer of direct tension to the matrix, when the fiber fails, resulting in local cleavage. In a more heavily reinforced composite a broken fiber transmits load to adjacent fibers primarily through shear in the matrix with more likelihood of local shear cracks or debonding. These local shear fractures are widespread and eventually link up to form the longitudinal cracks.

4. A comparison of fundamental fracture mechanisms between treated and untreated fibers in the same resin shows that a stronger bond is achieved with the treated fibers. This is particularly evident in the Type A fibers where untreated fibers failed and debonded for the most part, while surface treated Type A fibers generated matrix tensile cracks due to high shear concentrations at the newly formed ends.

5. Individual carbon fiber fractures are not sufficiently energetic to induce lower frequency signals as observed with boron filament specimens. These lower frequency events were believed to be due to specimen vibration but carbon fiber fractures result in acoustic signals having frequencies closer to the resonant frequency of the transducer.

6. Acoustic emissions show that specific failure events begin at approximately 50% of ultimate load for both HT and Type A fibers regardless of the epoxy resin formulation used. Since the crack sensitivity of the two resin formulations is quite different and the interfacial behavior of the two fibers is different, we conclude that these emissions must be primarily fiber fractures.

7. The acoustic emission rate is essentially the same for Type A fibers in both the modified and unmodified epoxy resin. This leads to the tentative conclusion that the failure process in these equivalent volume fraction composites is the same in each system.

During the remainder of this year additional acoustic emission data will be obtained for HT fibers in both modified and unmodified epoxy. Comparisons will also be made between acoustic emissions from high and low volume fraction composites to correlate with bulk strength data. Finally, failure processes will be analyzed in the composite/metal specimens which are now being prepared.

ACKNOWLEDGEMENTS

Acknowledgement is given to E. Muziani and R. Grosso for their efforts in preparation and testing of specimens. Dr. E. Feingold and E. Castagliuolo prepared photos of the fiber surfaces. The authors also wish to thank B. G. Achhammer and J. J. Gangler for their helpful technical suggestions.

REFERENCES

1. A. Gatti, et al, "Investigation of the Reinforcement of Ductile Metals with Strong, High Modulus Discontinuous, Brittle Fibers," Final Report NASw-1543, November 1967.

2. W. R. Tyson and G I. Davies, "A Photoelastic Study of the Shear Stresses Associated with the Transfer of Stress During Fibre Reinforcement," British Journal of Applied Physics, Vol. 16 (1965).

3. D. M. Schuster and E. Scala, "The Mechanical Interaction of Sapphire Whiskers with a Birefringent Matrix," Transactions of the Metallurigical Society of AIME Vol. 230, December 1964.

4. D. H. Johnson and C. N. Tyson, British Journal of Applied Physics (J. Phys. D.), 2, 787 (1969).

5. W. Ruland, J. Polymer Science, No. 28, Part C, 143 (1969).

6. R. G. C. Arridge, "Mechanical Properties of Fibre Reinforced Resins-Part 2 - A Theory of Fracture of Fibre Reinforced Viscoelastic Materials," University of Oxford, Oxford, England, 1969 Report No. 1084/69, U.S. Department of Commerce/N.B.S. Report N70-26202.

7. J. M. Hedgepeth, NASA Technical Note D-882, "Stress Concentrations in Filamentary Structures," May 1961.

8. Kaiser, J., "Erkenntnisse und Folgorungen aus dor Messung von Gerauschen bei Zugbeans pruchung von metallischen Workstoffen," Arch. Eisenhutt Wes. 1, 43 (1953).

9. Schofield, B.H., "Acoustic Emission under Applied Stress," ARL-150 (1961).

10. Liptai, R. G., et al, "Acoustic Emission Techniques in Materials Research," Univ. of California, Lawrence Radiation Laboratory, Report UCRL-72582, Sept. 1970.

11. Tatro, C.A.,"Experimental Considerations for Acoustic Emission Testing," Mat. Des. and Stds, 11, 17 (1971)

12. Mullin, J. V., Berry, J.M., and Gatti, A., Some Fundamental Fracture Mechanisms Applicable to Advanced Filament Reinforced Composites," J. Comp. Mat. 2, 82, (1968).

13. Mullin, J. V., Mehan, R. L., "Prediction of Composite Materials Performance through Acoustic Emission Analysis," to be published.